RANDOMLY OPTICAL SIGNALS GENERATED BY OPTICAL DEVICE FOR COMMUNICATION SECURITY

PAIBOON PONGWONGTRAGULL

A THESIS SUBMITTED IN FULFILLMENT

OF THE REQUIREMENT FOR THE DEGREE OF

DOCTOR OF PHILOSOPHY IN APPLIED PHYSICS

FACULTY OF SCIENCE

KING MONGKUT'S INSTITUTE OF TECHNOLOGY LADKRABANG

2011

KMITL-2011-SC-D-030-032

หัวข้อวิทยานิพนธ์	การสร้างสัญญาณทางแสงแบบสุ่มโดยใช้อุปกรณ์ทางแสงเพื่อใช้กับความปลอดภัยในการสื่อสาร
นักศึกษา	นายไพบูลย์ พวงวงศ์ตระกูล
รหัสประจำตัว	52650102
ปริญญา	ปรัชญาดุษฎีบัณฑิต
สาขาวิชา	ฟิสิกส์ประยุกต์
พ.ศ.	2554
อาจารย์ที่ปรึกษา	รองศาสตราจารย์ ดร. ปรีชา ยุพาพิน

บทคัดย่อ

วิทยานิพนธ์ฉบับนี้ นำเสนอเทคนิคการเข้ารหัสทางแสงแบบสุ่ม 2 ระบบ เพื่อใช้ในการประยุกต์ใช้งานด้านความปลอดภัยในการสื่อสาร ซึ่งสัญญาณแบบสุ่มสามารถนำมาสร้างเป็นสัญญาณที่เข้ารหัสได้ โดยในระบบแรก จะป้อนโซลิตอนแบบดาร์ค-ไบร์ตเป็นอินพุตเข้าไปในแมคเซห์นเดอร์อินเตอร์ฟีรอมิเตอร์ โดยที่คู่ของโซลิตอนแบบดาร์คและไบรต์จะเกิดขึ้นพร้อมกันโดยการใช้ตัวเลื่อนเฟสขนาด $\pi/2$ (อย่างเช่น กระจกแยกลำแสง) ซึ่งหมายความว่า จะใช้สถานะ $|D\rangle$ และ $|B\rangle$ แทนพัลซ์โซลิตอนแบบดาร์คและไบร์ตที่ตั้งฉากกัน ซึ่งสัญญาณจากพอร์ต Th จะถูกส่งไปในสายส่งไปยังผู้รับปลายทาง และจะใช้ฟิลเตอร์แบบแอด/ดรอปในการแยก (หรือกรอง) สัญญาณที่ต้องการออกมาจากสายส่ง สัญญาณจากพอร์ต Th จะใช้เป็นสัญญาณที่ส่งตามสายส่ง ส่วนพอร์ต Drop ใช้เป็นสัญญาณอ้างอิง นอกจากนี้การใช้พฤติกรรมของเฟสที่ต่างกัน $\pi/2$ ระหว่างโซลิตอนแบบดาร์คและแบบไบร์ตนี้ ก็จะเป็นพฤติกรรมเช่นเดียวกับพฤติกรรมของคู่โฟตอนที่เอ็นแทนเกิลกัน ซึ่งสามารถนำไปประยุกต์งานกับใช้กับข่าวสารเชิงควอนตัมได้ต่อไป โดยข้อดีของระบบนี้ คือ ระบบจะเป็นระบบที่ปลอดภัย สร้างง่าย และไม่ซับซ้อน

ระบบที่สอง เป็นการสร้างสัญญาณของการกระจายกุญแจรหัสลับเชิงควอนตัม ซึ่งสร้างโดยการใช้หน่วยความจำทางแสงแบบหลายช่องในการสร้างสัญญาณแบบสุ่มขึ้นมา โดยระบบของหน่วยความจำทางแสง จะถูกสร้างโดยการใช้ท่อนำคลื่นที่สร้างเป็นโพรงสั่นพ้องวงแหวนขนาดเล็ก โดยที่ระยะห่างระหว่างจุดยอดของแสงจะถูกสร้าง และเก็บไว้ภายในหน่วยความจำทางแสง ส่วนโพลาไรซ์โฟตอน จะถูกสร้างและจัดเก็บไว้ในอุปกรณ์เก็บข้อมูลทางแสง และส่งไปยังผู้ใช้ปลายทาง และถูกตรวจสอบโดยผู้ใช้ในแต่ละจุดภายในโครงข่าย ซึ่งโดยการใช้แนวความคิดของหน่วยความจำทางแสง ก็จะสามารถสร้างการกระจายกุญแจรหัสลับเชิงควอนตัมแบบต่อเนื่องหลายค่าได้ นอกจากนี้ ก็จะสามารถทำการส่งรหัสย่อเชิงควอนตัมผ่านช่องทางแบบมัลติเพล็กซ์ทางเวลา

ได้ ประโยชน์ของระบบนี้ คือ สามารถสร้างโครงข่ายที่ปลอดภัยโดยการใช้การกระจายกุญแจรหัสลับเชิงควอนตัมที่มีความจุ และความปลอดภัยสูง ซึ่งสามารถนำไปใช้ในโครงข่ายสาธารณะได้ต่อไป

Thesis Title	Randomly Optical Signals Generated by Optical Device for Communication Security
Student	Mr. Paiboon Pongwongtragull
Student ID	52650102
Degree	Doctor of Philosophy
Program	Applied Physics
Year	2011
Thesis Advisor	Assoc. Prof. Dr. Preecha Yupapin

ABSTRACT

In this thesis, we present the use of two different optical randomly encoded techniques for communication security applications, in which the random signals can be generated and formed the security encoded signals. In the proposed system, firstly, a dark-bright soliton pair is input into an optical Mach Zehnder interferometer (MZI), where the coincidence dark and bright soliton pair is occurred and obtained by using a $(\pi/2)$ phase retarder (i.e. a beamsplitter), which means that the $|D\rangle$ and $|B\rangle$ states represent the orthogonal dark and bright soliton pulses. The signals from through (Th) port are formed and transmitted to the transmission line and finally to the end user. The add/drop filter is used to separate (filter) the required signal form the transmission link, in which the Th and drop port signals are formed as transmitted and referencing signals, respectively. Moreover, because of the lack of phase of $(\pi/2)$ between dark and bright solitons, the use of such behaviors can form in the same way as the entangled photon behaviors, in which the use of dark-bright soliton pairs for quantum information applications can be realized. The advantage of such a system is that the system is secured, easily created and uncomplicated.

Secondly, a simultaneous generation of dense quantum key distribution is formed via an optical memory array to generate the random signals. The optical memory system is formed by using an array waveguide incorporating a nano ring resonator, whereas the different spatial light modes can be generated and stored within an optical memory unit. The polarized photon is formed and stored within a storing device, whereas the different time slot entangled photons can be generated, transmitted and detected by the different subscriber in the distributed networks. By using the optical memory concept, the continuous variable quantum key distribution is provided.

Furthermore, the use of quantum dense coding (QDC) via time division multiplexing paths is also plausible. The advantage of the proposed system is that the quantum key distribution can provide the network security with high capacity and safety, which is the large demand of usage in the public networks.

ACKNOWLEDGEMENTS

This thesis would not have been possible without the help, support and patience of my advisor, Assoc. Prof. Dr. Preecha Yupapin. I would like to express my greatest gratitude and thankfulness to him, for his generous support and guidance. His broad vision and remarkable knowledge of many fields of research, has proved to be invaluable in defining my research.

I would like to thank my co-workers at the Nanoscale Science and Engineering Research Alliance (N'SERA) and the Hybrid Computing Research Laboratory that have been key to this work, particularly Assoc. Prof. Dr. Somsak Mitatha, Dr. S. Suchat, Dr. N. Pornuwancharoen, Dr. S. Chaiyasoonthorn, Dr. N. Sangwara, Dr. S. Thongmee and especially Chat Teeka for all the support they gave me. Thanks are also due to friends and everyone for their conversation and helping everything.

Finally, I would like to thank my parents and my family for all their love and support.

Paiboon Pongwongtragull

CONTENTS

CONTENTS (Cont.)

CONTENTS (Cont.)

LIST OF FIGURES

Figures **Pages**

LIST OF FIGURES (Cont.)

Figures **Pages**

CHAPTER 1

INTRODUCTION

1.1 Motivation

From the pass till now, many forms of communication systems have been devised for sending messages from one place to another. The basic motivations behind each new form were to improve the transmission fidelity, to increase the data rate and to enhance the transmission distance between broadcast stations [1]. One of them is the use of light as the transmission medium for telecommunication which is called optical communication. In this form of communication, a transmitter encodes a message into an optical signal, which is transported to a receiver through a channel. The receiver reproduces the message from the received optical signal to its original understandable form.

Communication has become the important media and role in human daily life, in which the required communications in both wire and wireless communications [2, 3] must be fast and high security, therefore, the searching for new communication schemes still remains. Till date, many research works have been continuingly developed to increase in both speed and high security [4-6].

Dark and bright soliton behaviors have been widely investigated in different forms [7, 8]. The use of soliton, i.e. bright soliton in long-distance communication link has been implemented for nearly two decades, however, the interesting works using bright soliton in communication remain, whereas the use of soliton pulse within a micro ring resonator for communication security has been studied [9]. The interesting results are when the technique could be implemented within a tiny device such as a micro ring and a nano ring resonators and could be implemented within the mobile hand-set [9, 10]. The dark soliton is one of the soliton properties, whereas the soliton amplitude is vanished or minimized during the propagation in media, therefore, the dark soliton detection is difficult. The investigation of dark soliton behaviors has been reported [11, 14], where one point of them has shown interesting results, where the dark soliton can be stabilized [15] and converted into bright soliton [16] and finally detected. This means that we can use the dark soliton penalty due to the low level of the peak power to be the benefit, where the promising idea is that a dark soliton can performed the communication transmission carrier where the recovery can be retrieved by the dark–bright soliton conversion. Actually, we are looking for the

simple technique that can be employed to detect the dark soliton. Yupapin and Suwancharoen [17] have reported the interesting results of light pulse propagating within a non-linear micro ring device, where the transfer function of the output at the resonant condition is derived and used. They found that the broad spectrum of light pulse can be transformed to the discrete pulses.

Quantum network has also been introduced and has become the promising technology that can be used to fulfill the perfect network security. Some research works have been reported in various forms of applications [18, 19]. The use of quantum key distribution via optical network has been reported [20, 21]. To date quantum key distribution (QKD) is the only form of information that can provide perfect communication security. The use of QKD has been proposed in many research works, whereas the applications in different forms – such as point-to-point link [22], optical wireless [23], satellite [24], long distance [25] and network [26] – have been reported. However, a more reliable system for network security is needed, which is both high capacity and secure. The concept of continuous variable in the form of dense wavelength multiplexing is introduced to overcome such a problem. By using the continuous variable concept, the continuous QKD can be formed and available for a large demand. There are some works that have proposed the use of continuous variable QKD with quantum router and network [27, 28]. However, the requirement for large bandwidth signal and dense wavelength multiplexing has become the practical problems.

Quantum information was theoretically well established by Bennett et al. [29], who proposed a scheme that presented the use of quantum cryptography. The area of this research is now popularly investigated in either theoretical [30] or experimental [31] works, which is expected to have an implemented system for a wide range of application in the near future. To date, the demand of using the mobile telephone is still large. However, there is a serious problem of interception, where perfect security is greatly required from the users. The idea of quantum telephone has now become the key investigation. Many applications can be provided by the network providers. Furthermore, there are some advantages such as small size, lightweight and, especially, low cost. There is no such perfect security system that can secure the personal data should use the word safely from an eavesdropper that has been implemented in the telephone networks. Yupapin and Suchat [32] have reported the use of weak light to form a nonlinear behavior instead of using strong light pulse in an ordinary single-mode fiber, where the four-wave mixing result from the delayed pulse trains in the fiber ring resonator could be performed instead of the Kerr effect types in a fiber ring resonator. When the delayed polarization modes via the

ring resonator [33] were combined with the incoming light pulse trains, the entangled photon states were observed. In practice, this simple design and arrangement can be used as the quantum device for mobile telephone and network to be realistic. Recently, Suchat et al. [34] have proposed the promising concept of quantum key distribution via an optical wireless communication link for telephone networks. Manderbach et al. [35] have reported on the experimental implementation of a Bennett–Brassard 1984 (BB84) protocol-type quantum key distribution over a 144 km free-space link using weak coherent laser pulses. Fietz and Shvets [36] have reported that the generation of quantum key via a micro ring device is plausible, which means the use of quantum key within the telephone hand set will be realized in the near future.

In this thesis, we present the use of two different optical randomly encoded techniques for communication security applications, in which the random signals can be generated and formed the security encoded signals. In the proposed systems, firstly, a dark-bright soliton pair is input into an optical Mach Zehnder interferometer (MZI) using the lack of phase of $(\pi/2)$ to generate the $|D\rangle$ and $|B\rangle$ states, in which the use of dark-bright soliton pairs for quantum information applications can be realized. The advantage of such a system is that the system is secured, easily created and uncomplicated. Secondly, a simultaneous generation of dense quantum key distribution is formed via an optical memory array to generate the random signals. The polarized photon is formed and stored within a storing device which is the optical memory. The advantage of the proposed system is that the quantum key distribution can provide the network security with high capacity and safety, which is the large demand of usage in the public networks.

1.2 Basic Optical Communication

There are many forms of optical communication, for example, the airplanes use the landing lights at airports to land safely, the heliograph uses a mirror to reflect sunlight to a distant observer, distress flares are used by mariners in emergencies and optical fibers can be used as a medium to transmit light and thus information in a distance.

The primary role of optical fibers has long been to transmit high-speed bit streams from point to point, between nodes in the network. Electronics at the nodes have processed and switched the signals, multiplexing or demultiplexing them to different data rates, directing them to different nodes. In essence one can view the telecommunications network as built of two main components: pipes, which transmit signals, and switches which process and direct the signals.

Fibers are representing the pipes for high-speed signals. The first big step towards optical networking was the advent of wavelength-division multiplexing (WDM). The initial attraction of WDM was its ability to multiply the capacity of a single fiber. Instead of carrying a single time-division multiplexed (TDM) channel at 2.5 to 10 Gbit/s or even more, a fiber could carry 4, 8, 16, 32, 40 or more optical channels at different wavelengths, each may be at a different data rate. WDM makes signal management and processing possible on the wavelength level. Combing four 10 Gbit/s signals into a single 40 Gbit/s data stream requires an expensive electronic TDM multiplexer and a 40 Gbit/s optical transmitter including a receiver and demultiplexers to pick out one of the signals. If the four 10 Gbit/s signals are sent on separate optical channels, a filter can pick off the desired optical channel without disturbing the rest of the channels. This principle is applied in any WDM system: optical filters are used for separating one optical channel from the combined signal without electronics. Optical filters are key devices for WDM systems. The most obvious application is for demultiplexing very closely spaced channels, however, they also play major roles in gain equalization and dispersion compensation. [37]

1.3 Goal of the Thesis

The primary goal of this thesis is to investigate the design and simulation nonlinear characteristics of ring resonator architectures. The second goal is to understand the principle of optical devices. The third goal is to understand and design the quantum security and quantum key distribution using optical memory array. Finally, we can design a new system of dark-bright soliton conversion for the optical communication security system using the Mach Zehnder interferometer.

1.4 Scope of the Thesis

Scope of this thesis, we purpose the use of two different optical randomly encoded techniques for communication security applications using the optical devices, such as ring resonators, add/drop filters and Mach Zehnder interferometer, in which the random signals can be generated and formed the security encoded signals. And we also show the advantage of these techniques.

1.5 Organization of the Thesis

Chapter 1, introduction to the subject of the thesis, basic optical communication.

Chapter 2, descriptions of theoretical foundation nonlinear optics, optical ring resonators, optical add/drop filter and other optical filters.

Chapter 3, generation of polarized soliton pulses, continuous variable quantum key distribution, and entangled photons.

Chapter 4, descriptions of optical memory array and communication security using quantum key distribution.

Chapter 5, conversion of the dark-bright soliton using Mech Zehnder interferometer for optical communication security.

Chapter 6, conclusion and future works.

CHAPTER 2

THEORETICAL BACKGROUND

For an understanding of the theoretical foundation, the nonlinear optic and optical devices are described thoroughly in this chapter. Firstly the introductions to the nonlinear optics, such as nonlinear susceptibility, nonlinear refraction, self-phase modulation, cross-phase modulation, four wave mixing, optical chaos, optical bistability, optical chaotic communication and optical soliton, are shown in 2.1 – 2.10, respectively. In later sections, the optical ring resonators and optical add/drop filter are discussed in section 2.11 – 2.17, respectively. Finally, section 2.18, the optical filters are shown.

2.1 Nonlinear Susceptibility

Nonlinear optics is the study of phenomena that occur as a consequence of the modification of the optical properties of a material under intense illumination. Typically, only laser light is sufficiently intense to modify the optical properties of a material. Nonlinear optical phenomena are *nonlinear* in the sense that the induced material polarization is nonlinear in the electric field [38]. The general equation that describes the optical field evolution in a dielectric material is given by

$$\nabla^2 E - \frac{1}{c^2}\frac{\partial^2 E}{\partial t^2} = -\mu_0 \frac{\partial^2 P(E)}{\partial t^2} \tag{2.1}$$

where the polarization $\vec{P}$ characterizes the medium and it is a function of the electric field. In the case of weak nonlinear behavior of the medium, the polarization can be expressed by a Taylor polynomial as

$$\vec{P} = \underbrace{\varepsilon_0 \vec{E} + \varepsilon_0 \chi^{(1)} : \vec{E}}_{\text{linear PL}} + \underbrace{\varepsilon_0 \chi^{(2)} :: \vec{E}\cdot\vec{E} + \varepsilon_0 \chi^{(3)} ::: \vec{E}\cdot\vec{E}\cdot\vec{E} + \ldots}_{\text{nonlinear PNL}}, \tag{2.2}$$

where dielectric dispersion is ignored. $\chi^{(1)}$ is the linear susceptibility, :represents the inner tensor product and the second and the third-order tensor $\chi^{(2)}$ and $\chi^{(3)}$ are responsible for the second harmonic generation, and the third-order harmonic generation, respectively.

2.2 Nonlinear Refraction (Optical Kerr Effect)

The optical Kerr effect (i.e. nonlinear refraction index) results from the third order nonlinear susceptibility $\chi^{(3)}$, which is a fourth rank tensor.

An optical wave is a real quantity and usually expressed as

$$\vec{E}(t) = \mathrm{Re}\left\{\vec{E}e^{j(\vec{k}\cdot\vec{r}+\omega t)}\right\} \tag{2.3}$$

or similarly as

$$\vec{E}(t) = \frac{1}{2}\vec{E}e^{j(\vec{k}\cdot\vec{r}+\omega t)} + \text{c.c.} \tag{2.4}$$

where c.c. represents the complex conjugate of the preceding term. Thus, an x-polarized optical wave, propagating in the z-direction in an isotropic medium, is represented mathematically as

$$\vec{E}(t) = \frac{1}{2}E_x\hat{x}e^{j(kz+\omega t)} + \text{c.c.} \tag{2.5}$$

The third order polarization (mediated by $\chi^{(3)}$) in a material leads to a nonlinear intensity dependent contribution to its refractive index; i.e., the refractive index of the material changes as the incident intensity on the material changes. The susceptibility tensors in isotropic material can be further simplified as $\chi^{(2)} = 0$, due to inversion symmetry; the third order nonlinear susceptibility will only have one contributing term χ_{xxxx} since the light is x-polarized and there are no means for sourcing additional polarization components.

The linear and nonlinear induced polarizations are

$$P_L = \varepsilon_0(1+\chi^{(1)})E \tag{2.6}$$

and

$$\begin{aligned} P_{NL} &= P^{(3)} \\ &= \varepsilon_0\chi_{xxxx}(\omega;-\omega,\omega,\omega)\dot{E}^{*}EE \\ &\quad +\varepsilon_0\chi_{xxxx}(\omega;\omega,-\omega,\omega)EE^{*}E \\ &\quad +\varepsilon_0\chi_{xxxx}(\omega;\omega,\omega,-\omega)EEE^{*} \\ &= 3\varepsilon_0\chi_{xxxx}|E|^2E \\ &= \frac{3}{4}\varepsilon_0\chi_{xxxx}|E_x|^2E \end{aligned} \tag{2.7}$$

respectively. Hence,

$$P = P_L + P_{NL} = \varepsilon_0\left(1+\chi^{(1)}+\frac{3}{4}\varepsilon_0\chi_{xxxx}|E_x|^2\right)E$$

The total dielectric constant

$$\varepsilon_r^{tot} = \varepsilon_r + \Delta\varepsilon_r$$

where $\varepsilon_r = 1+\chi^{(1)} = n_0^2$ and $\Delta\varepsilon = \frac{3}{4}\chi_{xxxx}|E_x|^2$ after comparing with the expression for P. The refractive index is related to the dielectric constant as:

$$n = \sqrt{\varepsilon_r+\Delta\varepsilon_r} \approx \sqrt{\varepsilon_r}+\frac{\Delta\varepsilon_r}{2\sqrt{\varepsilon_r}} = n_0+\frac{3\chi_{xxxx}}{8n_0}|E_x|^2 \tag{2.8}$$

The intensity dependent refractive index for a nonlinear material is given by

$$n = n_0 + n_2|E|^2 \tag{2.9}$$

Comparing Eq.(2.8) and Eq.(2.9), the nonlinear refractive index is directly determined by the third-order susceptibility as

$$n_2 = \frac{3\chi_{xxxx}}{8n_0} = \frac{3\chi^{(3)}}{8n_0} \tag{2.10}$$

which characterizes the strength of the optical nonlinearity. The intensity I of an optical wave is proportional to $|E|^2$ as $I = \frac{1}{2\eta}|E|^2$ where η is the impedance of the medium. When comparing the optical response in the same medium, $I = |E|^2$ is taken for simplification.

2.3 Self-Phase Modulation

The change in refractive index due to the Kerr effect determines a corresponding change in the propagation constant. As a consequence, the phase of a signal propagating through the fiber varies with distance according to the equation:

$$\phi = n_0 k_0 z + \gamma P(t) z \tag{2.11}$$

where $\gamma = n_2 k_0 / A_{eff}$. The first term in Eq. (2.11) represents the linear phase shift due to signal propagation; the second term represents the nonlinear phase shift. When the incident wave is a pulse with a power variation given by $P(t)$, the output pulse is chirped. This phenomenon is called self-phase modulation (SPM), since the power variation within the pulse leads to its own phase modulation. In the leading edge of the pulse, where $dP/dt > 0$, the instantaneous frequency is downshifted from the central frequency, whereas in the trailing edge, where $dP/dt < 0$, the instantaneous frequency is upshifted. The chirping due to nonlinearity leads to increased spectral broadening.

In the presence of dispersion, the spectral broadening due to self-phase modulation determines two situations qualitatively different. In the normal dispersion region (where the wavelength is shorter than the zero dispersion wavelength, λ_{ZD}) the chirping due to dispersion is to downshift the leading edge and to upshift the trailing edge of the pulse, which is a similar effect as that due to self-phase modulation. Thus, in this regime the chirping due to dispersion and self-phase modulation add. On the other hand, in the anomalous dispersion region, the chirping due to dispersion is opposite to that due to self-phase modulation. Consequently, nonlinearity and dispersion induced chirpings can partially or even completely cancel each other. When this cancellation is total, the pulse neither broadens in time nor in its spectrum and such pulse is called a soliton. Much research effort has been devoted to the study of optical solitons and their application in telecommunication systems because they have the peculiar behaviors of preserving their shape during propagation [39, 40].

2.4 Cross-Phase Modulation

When two or more signals having different carrier frequencies are transmitted simultaneously inside an optical fiber, the nonlinear phase evolution of the signal at frequency ω_i depends also on the power of the other signals. This nonlinear phenomenon is known as cross-phase modulation (XPM) and it is due also to the intensity dependence of the refractive index. The nonlinear phase shift of the signal at ω_i becomes:

$$\phi_i^{NL} = \gamma z\left[P_i + 2\sum_{i\neq j} P_j\right] \tag{2.12}$$

Where $P_{i,j}$ is the power of the signal at $\omega_{i,j}$. The first term in the square brackets represents the contribution of self-phase modulation, while the second term is the contribution from the cross-phase modulation. The factor 2 in Eq. (2.12) indicates that cross-phase modulation is twice as effective as self-phase modulation for the same amount of power.

From Eq. (2.12) it can be deduced that cross-phase modulation is effective only when the interactive signals are superimposed in time. In the presence of finite dispersion, two pulses at different frequencies will move with different velocities and thus the pulses will walk off from each other. Obviously, larger dispersion will reduce the walk off length and hence the cross-phase modulation effects.

Due to cross-phase modulation, the phase of each channel in a WDM system is affected by both the average power and the bit pattern of all other channels. Fiber dispersion converts phase variations into amplitude fluctuations that affect the signal-to-noise ratio (SNR) and introduce jitter. In these circumstances, an understanding of the interplay between cross-phase modulation and group velocity dispersion is very important for WDM systems [41].

2.5 Four Wave Mixing

When the signal at difference frequencies propagates through the medium, besides cross-phase modulation, another important effect occurs: four-wave mixing (FWM) [42].

Four-wave mixing is a nonlinear effect arising from a third-order optical nonlinearity, as is described with a $\chi^{(3)}$ coefficient. It can occur if at least two different frequency components propagate together in a nonlinear medium such as an optical fiber. Assuming just two input frequency components ω_1 and ω_2 (with $\omega_2 > \omega_1$), a refractive index modulation at the difference

frequency occurs, which creates to additional frequency components (Fig 2.1). In effect, two new frequency components are generated:

$$\omega_3 = \omega_1 - (\omega_2 - \omega_1) = 2\omega_1 - \omega_2 \text{ and } \omega_4 = \omega_2 - (\omega_2 - \omega_1) = 2\omega_2 - \omega_1$$

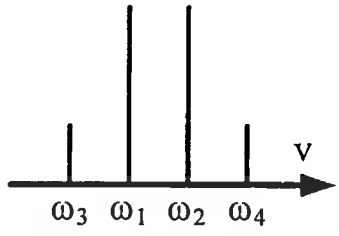

Fig. 2.1 Generation of new frequency components via four-wave-mixing.

Four-wave mixing is a parametric interaction among waves satisfying a given phase relationship called phase matching. Different phenomena may be originated by four-wave mixing process depending on the relation among interaction frequencies. If three optical fields with carrier frequencies ω_i (i = 1, 2, 3) co propagates inside the medium simultaneously, it appears that the third-order polarization vector has several components: three components have the frequencies of the input fields, the others have an angular frequency ω_4 given by

$$\omega_4 = \omega_1 \pm \omega_2 \pm \omega_3 \tag{2.13}$$

If no field is present in the medium at the frequency ω_4, a new field component is created at this frequency. If a field at the frequency ω_4 is already present in the medium, it will be affected by the nonlinear interaction between the fields at ω_i, which causes crosstalk in multi-channel communication systems.

The phase-mismatch among all for waves is given by

$$\Delta\beta = \beta(\omega_1) + \beta(\omega_2) - \beta(\omega_3) - \beta(\omega_4) \tag{2.14}$$

Where $\beta(\omega)$ is the propagation constant for an optical field with frequency ω. Assuming that the frequencies to be closely and equally spaced (i.e., $\omega_1 = \omega_2 - \Delta\omega$, $\omega_3 = \omega_2 - 2\Delta\omega$, $\omega_1 = \omega_2 - \Delta\omega$) and making a Taylor series expansion of all βs about the frequency ω_2, we get

$$\Delta\beta = 2\beta_2(\Delta\omega)^2 \tag{2.15}$$

where $\beta_2 = \partial^2\beta/\partial\omega^2$ is the group velocity dispersion (GVD). When $\beta_2 = 0$ we a perfect shave-phase matching and thus an efficient four-wave mixing. This situation is desirable for applications such as all-optical signal processing, wavelength conversion, pulse compression, etc. four-wave mixing in optical materials can also be used for generating spectrally inverted signal through the process of optical phase conjugation (OPC), which is useful for dispersion compensation. However, in WDM systems four-wave mixing causes a transfer of power from each channel to its neighbors. Such a power transfer not only results in the power loss for the channel but also induces inters channel crosstalk that degrades the system performance severely. This problem can be minimized using the technique of dispersion management, in which the dispersion is kept locally high even though it is low on average.

2.6 Optical Chaos

Optical Chaos is observed in many nonlinear optical systems. One of the most common examples is a ring resonator. One of the most seminal works is published by Ikeda (Physical Review Letters, 1982) where chaotic behavior in a ring resonator was proposed and experimentally confirmed. Optical Chaos was an exciting field of research in mid-1980s and was expected at that time to lead to production of all optical devices including all optical computers. Researchers realized later the inherent limitation of the optical systems due to the non-localized nature of photons compared to highly localized nature of electrons. Research in Optical Chaos has seen a recent resurgence in the context of studying synchronization phenomena, and in developing techniques for secure optical communications. [43-44]

2.7 Optical Bistability

The phenomenon of optical bistability (OB) arises from a combination of the nonlinearity in the radiation-matter interaction and of a feedback mechanism [45-47]. Generally, there are two classes of optical bistability: absorptive and dispersive optical bistability. Absorptive optical bistability occurs whenever the input wavelength is close to the atomic resonance of the material. An increase in the input power produces an increase in saturation, i.e., in the degree of transparency of the medium. This allows the internal field of the cavity to increase, which in

return increases the saturation. Such positive feedback loop causes the switch-up process. When the input power is decreased, the internal field is intense enough to maintain the saturation. As a consequence, the transmitted power is held "ON" and one obtains a hysteresis curve. InGaAsP can be designed to have the band edge around 1.45 μm and thus can show absorptive optical bistability when pumped at 1.55 μm. On the other hand, dispersive optical bistability occurs whenever the input wavelength is tuned far away from the atomic resonance and hence the material is transparent. The frequency of the incident field is kept near one of the cavity frequencies, but detuned enough so that the transmission is low. An increase in the input intensity produces an increase in the intensity of the internal field. Because the refractive index is a function of intensity, this changes the optical length of the medium in such a way that the cavity resonance is driven closer to the input frequency. In return, it increases the internal field intensity. Thus, again, we have a positive feedback loop which produces up-switching. When the incident power is decreased, the internal field is intense enough to maintain resonance between the cavity and the input frequency, and therefore one again obtains a hysteresis. For example of this phenomena is shown in Fig. 2.2 which the input wavelength is at 1.55 μm. The characteristic of bistability hysteresis can be implemented as optical switching.

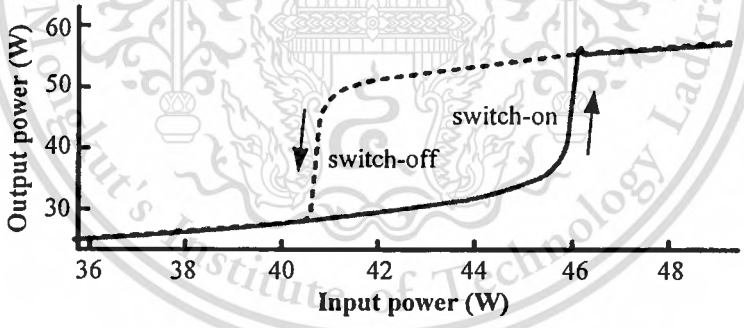

Fig. 2.2 The output power versus the input power showing the bistability hysteresis used as switch "on" and "off".

2.8 Optical Bifurcation

Bifurcation theory is the mathematical study of how and when the solution to a problem changes from there only being one possible solution, to there being two, which is called a bifurcation. Most commonly used in the mathematical study of dynamical systems, a bifurcation occurs when a small smooth change made to the parameter values (the bifurcation parameters) of

a system causes a sudden 'qualitative' or topological change in its long-term dynamical behavior. Bifurcations occur in both continuous systems and discrete systems. [48, 49]

The study of how the character of fixed points change as parameters of the system change is called bifurcation theory. (Recall that the term bifurcation is used to the describe any sudden change in the dynamics of the system. When a fixed point changes character as parameter values change, the behavior of trajectories in the neighborhood of that fixed point will change. Hence the term bifurcation is appropriate here.) Being able to classify and understand the various possible bifurcations is an important part of the study of nonlinear dynamics.

2.9 Optical Chaotic Communication

The appearance in the year of 1990 of two seminal papers involving fundamentals of chaotic systems to generated a tremendous amount of interest and work with subsequent applications in synchronization and control of chaos. In particular, the peculiar features of chaotic systems well explored [50, 51] (synchronization capability and sensitivity to initial condition), opened up a whole new field for using chaotic signals as information carriers. It is currently accepted that chaotic systems provide a rich mechanism for signal design and generation, with promising potential applications to communications and signal processing. Since chaotic signals are typically broadband, noise like and difficult to predict they can be used in various contexts for masking information-bearing waveforms. They can also be used as modulating waveforms in spread spectrum systems, like Code Division Multiple Access (CDMA) that is becoming very popular in many fields of telecommunication. Two fundamental characteristics of chaos in physical systems are the complexity of the dynamics and the sensitivity of the time evolution to small perturbations. The sensitivity of chaos to small perturbations has been seen for a long time as merely a barrier to prediction, and not as a useful property. Major developments in the area of controlling chaos using small perturbations have proved otherwise: the sensitivity to small perturbations exhibited by chaotic systems allows controlling them using.

Chaos communications is an application of chaos theory which is aimed to provide security in the transmission of information performed through telecommunications technologies. By secure communications, one has to understand that the contents of the message transmitted are inaccessible to possible eavesdroppers.

In chaos communications security is based on the complex dynamic behaviors provided by chaotic systems. Some properties of chaotic dynamics, such as complex behaviors, noise-like

dynamics (pseudorandom noise) and spread spectrum, are used to encode data. On the other hand, being chaos a deterministic phenomenon, it is possible to decode data using this determinism. In practice, implementations of chaos communications devices resort to one of two chaotic phenomena: synchronization of chaos, or control of chaos. The implement chaos communications using such properties of chaos, two chaotic oscillators are required as a transmitter (or master) and receiver (or slave). At the transmitter, a message is added on to a chaotic signal and then, the message is masked in the chaotic signal. As it carries the information, the chaotic signal is also called chaotic carrier.

When chaos synchronization is used, a basic scheme of a communications device (Cuomo and Oppenheim 1993) is made by two identical chaotic oscillators. One of them is used as the transmitter, and the other as the receiver. They are connected in a configuration where the transmitter drives the receiver in such a way that identical synchronization of chaos between the two oscillators is achieved. For the purpose of transmission of information, at the transmitter, a message is added as a small perturbation to the chaotic signal that drives the receiver. In this way, the message transmitted is masked by the chaotic signal. When the receiver synchronizes to the transmitter, the message is decoded by a subtraction between the signal sent by transmitter and its copy generated at the receiver by means of the synchronization of chaos mechanism. This works because, whilst the transmitter output contains the chaotic carrier plus the message, the receiver output is made only by a copy of the chaotic carrier without the message. The electrical signals with a power far below the one produced by the chaotic system itself. Thus, the complexity of chaos and its sensitivity to small perturbations can be combined harmoniously by using the sensitivity to control (and take advantage of) the complexity. As a consequence, it is currently recognized by many engineers that the fact that chaos provides complex behavior from simple systems can be exploited to obtain technological advantages over conventional means for information transmission.

Optical Chaos is observed in many nonlinear optical systems. One of the most common examples is a ring resonator. One of the most seminal works is published by Ikeda (Physical Review Letters, 1982) where chaotic behavior in a ring resonator was proposed and experimentally confirmed. Optical Chaos was an exciting field of research in mid-1980s and was expected at that time to lead to production of all optical devices including all optical computers. Researchers realized later the inherent limitation of the optical systems due to the non-localized nature of photons compared to highly localized nature of electrons. Research in Optical Chaos has

seen a recent resurgence in the context of studying synchronization phenomena, and in developing techniques for secure optical communications. [52, 53]

2.10 Optical Soliton

In a linear medium, the phase between the different plane waves depends solely on the propagation angle. It is clear then, that if all the plane wave components have the same angles, they will also have the same phase velocity and no phase difference will be acquire during propagation. If we represent the propagation direction of these plane waves by arrows, these arrows will creates a cone in space. The associated beam will propagate in this linear medium with no broadening while it maintain it's shape and dimensions. This type of beams is called "Bessel beams" since their field is described by Bessel function.

In a nonlinear medium, however, each plane wave is influenced by all the others. This is because the index change is a function of the total intensity. For some nonlinearities it is possible to find an ensemble of plane waves which will delay the phase velocity of the on axis components (in comparison with the of axis components). Consequently, the phase delay between the different propagating plane waves will be compensated by the other waves via the medium nonlinearity.

If the nonlinearity is such that the index at the beam center is higher than in the dark regions, then the plane wave that propagate on axis will experience the highest index and will propagate slower from those off axis. This high index experienced by the on axis wave can compensate for its linear tendency to propagate faster (because it is on axis). One example in which the index of refraction fully compensates for the shorter trajectory is a hyperbolic secant solution in a Kerr type medium. The plane waves that construct the hyperbolic secant index profile (induced by the beam via the nonlinearity) have all the same phase velocity along propagation, and hence their interference (the hyperbolic secant shape) also maintains its shape and size as it propagates.

One can also look on solitons from the mathematical perspective. One has to find a stationary wave solution of governing nonlinear wave equation. The mathematical aspects of solitons are out of the scope of this thesis. Hence, here we will give just the final solution. For the exact mathematical derivation, the reader may refer to [54-56].

We start from the Maxwell equations with the following assumptions:

- The electric field in the propagation direction is negligible in comparison with the transverse electric field (paraxial approximation).

- The electromagnetic wave is monochromatic and its frequency is ω.

- The transverse electric field is $E(x,y,z,t)=\psi(x,y,x)\exp[j(\omega t-kz)]$ where the slowly varying field $\psi(x,y,x)$ changes much slower than $\exp[j(\omega t-kz)]$.

- The change in the refractive index is much smaller than one.

For beams in Kerr type medium (for which the index of refraction is the following function of the intensity: $n(I)=n_0+n_2 I$, one can start from the Maxwell equations and derive the nonlinear Schrödinger equation:

$$\frac{\partial}{\partial z}\psi(x,y,z)=\left[\frac{j}{2k}\left(\frac{\partial^2}{\partial x^2}+\frac{\partial^2}{\partial y^2}\right)+\frac{jkn_2}{n_0}|\psi(x,y,z)|^2\right]\psi(x,y,x) \qquad (2.16)$$

Here, z is the propagation direction, k is the wave vector, and ψ is the slowly-varying amplitude of the electric field. Among all solutions for Equation (2.16) there is one family of particular interest:

$$\psi=\sqrt{\psi_0}\,\mathrm{sech}\left[\frac{x}{W_0}\right]\exp\left[j\left(\frac{z}{4z_0}\right)\right] \qquad (2.17)$$

Here $W_0=\sqrt{\frac{2n_0}{n_2}}\frac{1}{k\psi_0}$ and $Z_0=\frac{kW_0^2}{2}$. We can see that the intensity of this subfamily $I(x,y)=|\psi|^2$ is z independent. For any chosen peak power, ψ_0, we can find a sech solution with appropriate width (the width, W_0, is a function of the peak intensity and is wider for lower peak intensities). All solutions of this sub-family (equation (2.17)) will keep their shape and size invariant along propagation. Yet, in order to observe such solitons in nature, it is not enough to have a steady state mathematical solution in hand: one should also check for the stability of this steady state solution to noise and to deviations from ideal initial condition. If the solution exemplifies a state of stationary propagation-only then it can be considered as a soliton.

2.11 The Ring Resonator History

The proposal to use an integrated ring resonator for a band pass filter has been made in 1969 by E. A. Marcatili [57]. The layout of the channel dropping filter is shown in Fig. 2.3. The transmission properties of the used guide consisting of a dielectric rod with rectangular cross

section, surrounded by several dielectrics of smaller refractive indices have been described by E. A. Marcatili in [58].

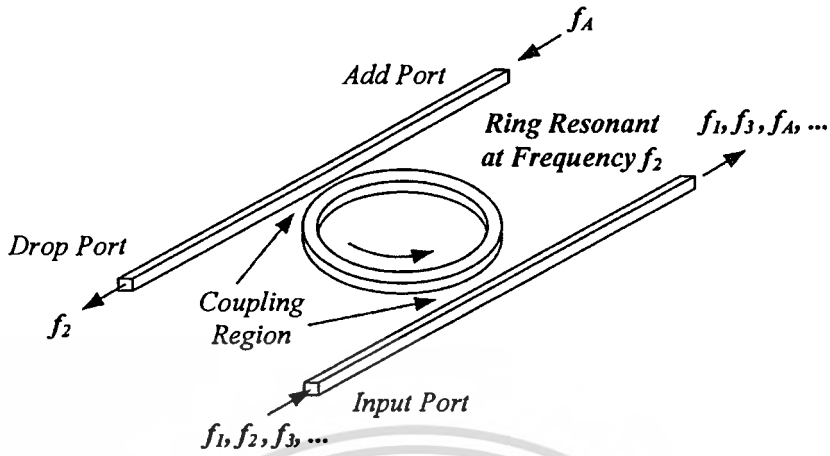

Fig. 2.3 Ring resonator channel dropping filter.

A general architecture for an autoregressive planar waveguide optical filter was demonstrated for the first time in 1996 [59]. The autoregressive lattice filters which were designed and fabricated consisted of one and two stages using Ge-doped silica waveguides.

A signal flow chart transformation for evaluating the filter transfer functions was demonstrated. Purely passive single ring resonator filters shown in Fig. 1.1 have been realized in the material system AlGaAs-GaAs [60, 61] and Si-SiO_2 [62] and Si_3N_4- SiO_2 [63]. The radius of the used ring resonators is between 5 μm and 30 μm and the free spectral range (FSR) achieved is between 20 nm and 30 nm. Passive ring resonators in the form of a racetrack have been realized in the material system GaInAsP [64] and AlGaAs-GaAs [65]. The filter performance is limited by bending and scattering losses in the resonator. These losses could be compensated by using or adding an active material.

2.12 Optical Add/Drop Ring Resonator Filter

A ring resonator consists of a waveguide in a closed loop. The loop can be any closed shape, such as a circle, ellipse, or racetrack. The ring is placed near one or two bus waveguides (Fig. 2.4). Typically, the input signal consists of one or more WDM channels. Signals on the input bus couple evanescently to the resonator. If a channel wavelength is resonant in the resonator, i.e., it encounters an integral multiple of 2π in phase over a round-trip, the signal intensity builds up in the ring, it couples to the output bus, and is "dropped". At the same time, a

signal on the same wavelength can be added via the add port. The resonator thus functions as an add/drop multiplexer.

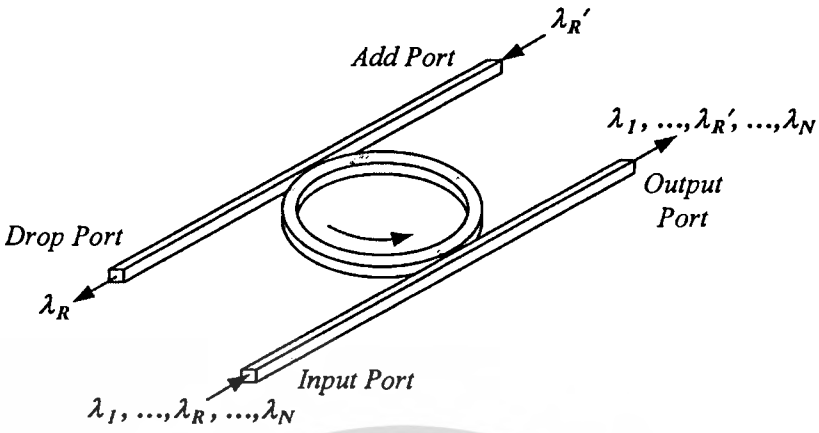

Fig. 2.4 Schematic diagram for a ring resonator coupled to two waveguides as an add/drop filter.

An incident optical signal composed of multiple wavelengths ($\lambda_1,...,\lambda_R,...,\lambda_N$) at the input port coupled into the ring and for a resonant wavelength (λ_R), the energy builds up in the resonator despite the small coupling and eventually the signal is coupled into the drop port. Symmetrically, a new signal at resonant wavelength (λ_R') at the add port couples to the output port through the ring. As a result, such a configuration constitutes a very compact add/drop filter where a channel can be dropped from the WDM spectrum and replaced by a new signal on the same channel. Note that waves with a wavelength away from resonance will not repeat themselves in the ring and the coupled field interferes destructively with the wave in the resonator leading to little energy in the resonator and little dropped power. Residual dropped power at non-resonant wavelengths is possible due to imperfections and can induce inter-band crosstalk that is detrimental to WDM applications. Moreover, if the input channel at λ_R is not completely extinguished, intra-band crosstalk will result. These issues will be studied and can be theoretically overcome by varying coupling parameters, inducing loss/gain in the ring and inserting additional rings between the two waveguides.

2.13 The Ring Resonator

A ring resonator is simply a waveguide shaped into a ring structure as shown in Fig. 2.5. When an input electric field, E_i is coupled to the ring waveguide through an external bus waveguide, a positive feedback is induced and the field inside the ring resonator, E_r starts to

build up. Coupling between the straight and the ring waveguide is achieved through the evanescent wave. Therefore, the gap and coupling length between them determine how much power is coupled from the straight waveguide to the ring waveguide and vise versa. The feedback mechanism is simply induced by the ring waveguide and therefore there is no need for any Bragg gratings, mirrors, or distributed feedback waveguides which are more difficult to fabricate. In such configuration, only certain wavelengths will be allowed to resonate inside the ring waveguide, thus frequency selectivity is obtained.

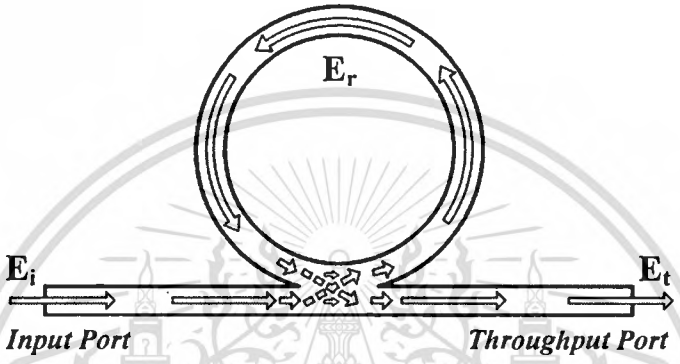

Fig. 2.5 Schematic diagram for a ring resonator coupled to a single waveguide.

A resonant mode will have a wavelength that satisfies.

$$m\lambda_m = nL\,,\ m = \text{integer} \tag{2.18}$$

Here, m is the longitudinal mode number, λ_m is the resonant mode wavelength, n is the refractive index of the guiding material, and L is the circumference of the ring resonator.

A ring resonator device is promising candidates for wavelength filtering, multiplexing/demultiplexing, conversion and network routing application. Two typical settings of ring resonator are shown in Fig. 2.6. A ring or a disk shaped dielectric cavity is placed between two parallel dielectric straight waveguides. In real life devices, the straight waveguides can be positioned either in the same plane (Fig. 2.6 (a) horizontal coupling scheme) or below (Fig. 2.6 (b) vertical coupling scheme) the cavity plane. These two straight waveguides form four ports for the external connections, the two input ports named "In-port" and "Add-port", and the two output ports named "Through-port" and "Drop-port". To understand the functioning of the ring resonator, for the sake of simplicity, let's consider only unidirectional fields (clockwise

propagating), where only the In-port is illuminated, while there is no incoming signal at the Add-port.

Conventionally, the functioning of ring resonator is described by the interaction of harmonic optical waves propagating along the straight waveguide and the cavity, and the interferometric resonances of the waves inside the cavity. A single frequency optical wave is launched at the In-port of the resonator. As this signal propagate s along the upper straight waveguide, that connects the In-port and Through-port, part of it is evanescently coupled to the cavity. While propagating along the cavity, part of this signal is coupled to the lower straight waveguide and appears at the Drop-port. The remaining part of the signal propagates along the cavity, and interferes with the newly in-coupled signal in the upper interaction region. Depending upon the specific configuration, these two fields undergo constructive or destructive interference.

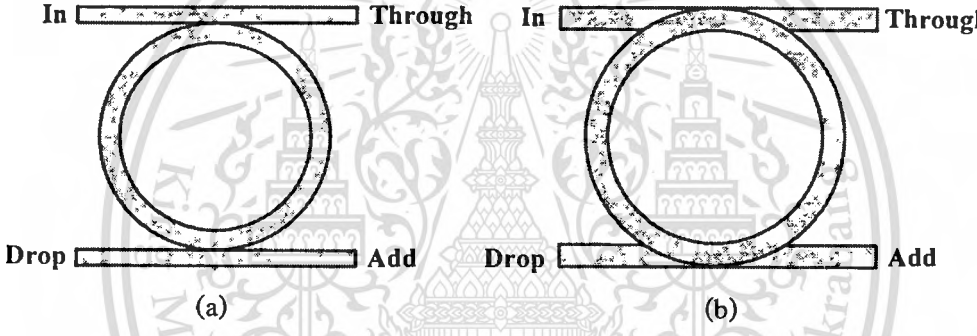

Fig. 2.6 Images of real life coupling ring resonator

(a) Horizontal coupling ring resonator (b) Vertical coupling ring resonator.

If the cavity field is out of phase with the newly entering field, then destructive interference takes place inside the cavity and as a result, there is only a small amount of power inside the cavity. Under so-called off resonance conditions, as shown in Fig. 2.7 (a), most of the input power is directly transmitted to the Through-port, and there is comparably low power at the Drop-port.

On the other hand, if the field inside the cavity is in phase with the newly in-coupled signal, then due to constructive interference, energy builds up inside the cavity. This field gets coupled to the Drop-port waveguide. Under so-called resonance conditions, there is a significant power observed at the Drop-port, while less power appears at the Through-port. This situation is shown in Fig. 2.7 (b).

A typical spectral response of a ring resonator device is shown in Fig. 2.7. Resonance appears as dips in the Through-port power curve and peaks in the Drop-port power curve. In other words, the wavelength for which ring resonator is on resonance, will be "dropped" at the Drop-port. Also, for a symmetrical device, if a new signal that corresponds to a resonance wavelength is launched at the Add-port, it will get "added" to the off resonance signal launched at the input port, and appears at the Throughput port. Therefore the arrangement shown in Fig. 2.8 can be used as an add/drop filter. [66]

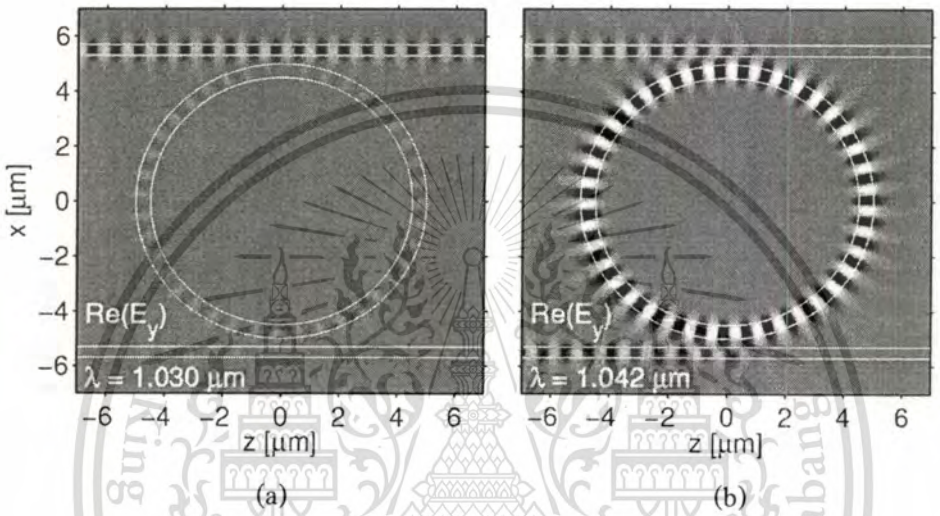

Fig. 2.7 Images of resonance state of a micro resonator (a) Off-resonance state (b) Resonance state. [66]

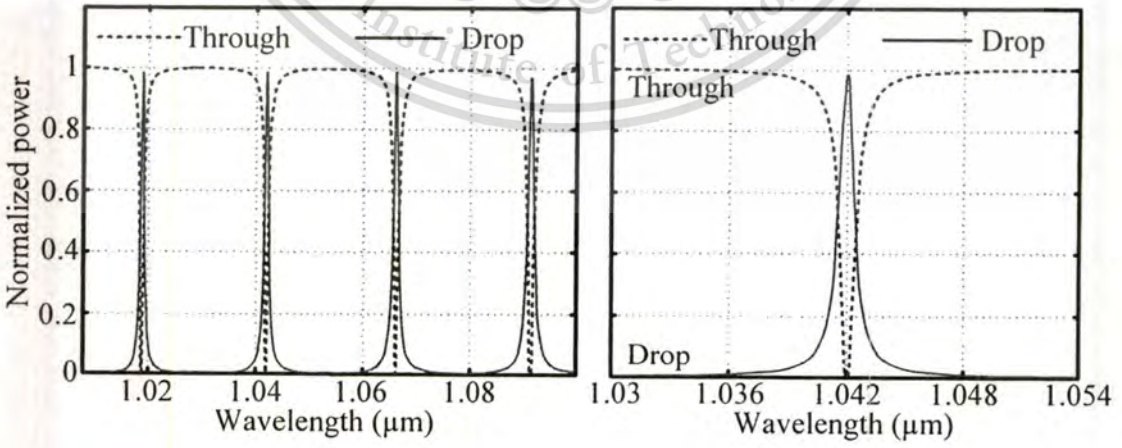

Fig. 2.8 Show the wavelength dependent response of the micro resonator as introduced in Fig. 2.7. [66]

2.14 Micro Ring Resonators

Now we can summarize the advantages attained by micro ring resonators over other conventional optical cavities:

- Geometry

The ring geometry by itself is unique. The ring waveguide supports a traveling wave rather than a standing wave. Hence, coupling can be at any point on the ring circumference. Furthermore, it allows more than one waveguide to be coupled to the ring. Therefore, multiplexing, demultiplexing, and routing can be achieved with no need for external circulators.

- Simplicity

Fabrication of micro ring resonators is straightforward. There is no need for any mirrors, Bragg gratings, or distributed feedback waveguides to achieve the positive feedback.

- Materials

There is no need for any exotic materials to fabricate micro ring resonators. Semiconductors fabrications are well developed and their high refractive indices allow smaller radii bends to be feasible. Bending losses decrease exponentially with increasing core-cladding refractive index contrast. This made high index contrast a fundamental requirement for very large scale integration (VLSI) photonics. A 2 μm micro ring resonator with a finesse of 100 will have a cavity lifetime of 10 ps. Therefore, 100 GHz data can be processed by such a device. Semiconductors also allow micro rings to be integrated with other optoelectronics devices such as microlasers, amplifiers, and detectors.

2.15 Integrated Ring Resonator System

The basic type of autoregressive moving average (ARMA) planar waveguide filter is a single ring resonator connected to one coupler provides no path back to the input port. This filter is called all-pass or, in the absence of loss, unit transmittance networks [67], because the magnitude of their transmission factor is unity on the whole spectrum, independent of wavelength. Although lossless all-pass filters do not display magnitude filter characteristics, their phase response is frequency dependent. Therefore, they can be configured for group delay equalization and dispersion compensation [68–70], polarization mode dispersion compensation [71], and other applications based on their phase-frequency characteristics such as band-pass filtering when used in conjunction with other optical components. There have been growing

interests in tunable dispersion compensators (TDC) for high-speed wavelength division multiplexed (WDM) networks. This is because the chromatic dispersion of transmission path could be changed frequently in a dynamically re-configurable WDM networks. The TDC based on ring resonator all-pass filter is one of the key components in these networks. Optical ring resonator all-pass filters (RRAPF) can be realized using multi-stage in either cascading single stages or using lattice architectures [65]. In this thesis, multi-stage ring resonator all-pass filters for dispersion compensation is proposed and analyzed. Desired group delay shape, which has a larger value and sharper, can be tuned by the amount of power coupling to the ring.

2.16 Behavior of Light in Ring Resonator

Optical soliton has been recognized as a nonlinear solitary wave for years. Since then, it has been widely investigated in several subjects such as in physics, mathematics and communication, especially, in optical communication. Generally, the common property of a soliton known as self-phase modulation and cross-phase modulation are the challenged behaviors. Furthermore, the non-dispersion behavior of the soliton is the key advantageous, which is capable the use in long-haul communication where the long distance link without a repeater can be employed. The other interesting soliton behavior is the localization where the soliton pulse can be trapped and stored within the periodic medium, which is useful in many areas of applications. Theoretically, a soliton pulse can be recovered when the balance between dispersion and nonlinear lengths of the soliton pulse exhibits the soliton behavior known as self-phase modulation, which it occurs when the matching between the soliton property and localized media is provided. When the generation of the localized soliton pulse is achieved, it is available for applications in many areas of research in science and technology. One of the interesting applications is that the high speed computer, i.e. quantum computer) which can be reversely processed. However, the problem remains where the memory for quantum computer is required, is the ability to drastically slow down the propagation speed of light, and to coherently stop and store optical pulses, hold the key to ultimate control of light. It has profound implication for optical communication [72] and quantum information processing [73, 74]. There are two major approaches, employing either electronics or optical resonant. However, most of the system imposes severe constraints. One of the recent works was reported, where the general analysis for the criteria to stop and store light coherently using array micro cavities (waveguides) was proposed by Yanik and Fan [75, 76]. They have shown that light could be stopped and stored coherently under adiabatic condition with

all optical system. However, the system is still complicated, which is difficult to make a realistic implementation. Therefore, the searching for the suitable devices and technologies are still necessary. Recently, the use of a chaotic soliton to form a fast light generation within a tiny device known as a micro ring resonator (waveguide) has been reported by Yupapin et al [77]. They have shown that the large bandwidth can be compressed coherently with a small group velocity. In practice, such devices have been fabricated and used in various applications [78-81]. In this thesis, we show that the large bandwidth of light pulse is generated and compressed within the nonlinear micro and nano ring system. The selected (tuned) pulse is coherently stopped and stored within the nano ring device. In applications, we can use the tuned light pulse to perform the required applications such as optical memory, quantum repeater and quantum logic gate. We have also discussed that when the coherent pulse is in the stopping situation, the output gain is constant, which is allowed to store light pulse to be stored coherently within the device.

2.17 The Ring Resonator – The Used Model

A single ring resonator is transferred into a box like filter shape using a single coupler or a double coupler configuration as shown in Figs 2.9 and 2.10. A calculation model is derived and all essential parameters describing the transmission characteristic are extracted in this section.

2.17.1 Single Coupler Ring Resonator Filter (SCRR)

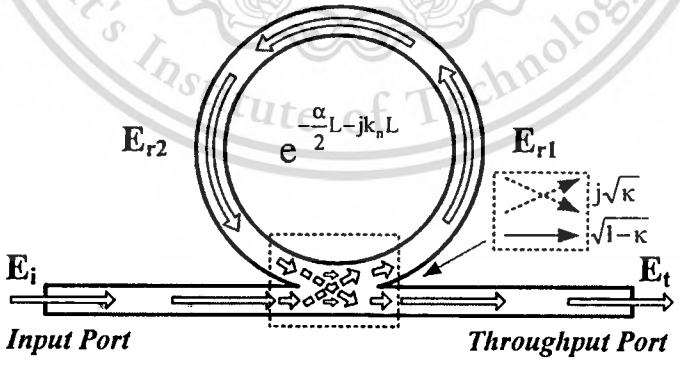

Fig. 2.9 Schematic diagram for a ring resonator coupled to a single waveguide.

The transfer function of this configuration is derived using Z-transform analysis. The circumference of the ring is L ($L = 2\pi R$, the radius is R), the coupling coefficient of the

coupler is κ. The Z-transform parameter is represented by $z^{-1} = \exp^{-jk_n L}$ where $k_n = \frac{2\pi}{\lambda} n_{eff}$ is the propagation constant and n_{eff} is the effective index of the waveguide. The one round trip loss is $a = e^{-\alpha L/2}$, α is the intensity attenuation coefficient inside the waveguide [unit length^{-1}]. γ is the fractional coupler intensity loss. The transmitted or throughput field at the output of the straight waveguide, E_t and inserted electric field, E_i relations can be derived as followed:

$$E_t = (1-\gamma)^{1/2} \times \left[E_i \cdot \sqrt{1-\kappa} + j \cdot E_{r2} \sqrt{\kappa}\right] \tag{2.19}$$

$$E_{r1} = (1-\gamma)^{1/2} \times \left[j \cdot E_i \cdot \sqrt{\kappa} + E_{r2} \cdot \sqrt{1-\kappa}\right] \tag{2.20}$$

$$E_{r2} = E_{r1} \cdot a\, z^{-1} \tag{2.21}$$

Using these equations, E_t / E_i can be calculated:

$$\frac{E_t}{E_i} = (1-\gamma)^{1/2} \times \left[\frac{\sqrt{1-\kappa} - (1-\gamma)^{1/2} \cdot a z^{-1}}{1 - (1-\gamma)^{1/2} \cdot \sqrt{1-\kappa} \cdot a z^{-1}}\right]. \tag{2.22}$$

The transfer function in Eq. (2.22) indicates that a ring resonator is very similar to a Fabry-Perot cavity. In the particular case shown in Fig. 2.9, the corresponding Fabry-Perot cavity would have an input mirror with a field reflectivity and a fully reflecting output mirror. However, the field propagating inside the ring cavity is a traveling wave in contrast to the Fabry-Perot cavity which resonates a standing wave.

In the following, new parameter will be used for simplification:

$$\begin{aligned} D &= (1-\gamma)^{1/2} \\ x &= D \cdot e^{-\alpha L/2} \\ y &= \sqrt{1-\kappa} \\ \phi &= k_n \cdot L \end{aligned} \tag{2.23}$$

The intensity relation for the output port is given by:

$$T = \frac{I_t}{I_i}(\phi) = \left|\frac{E_t}{E_i}\right|^2 = D^2 \cdot \left[1 - \frac{(1-x^2)\cdot(1-y^2)}{(1-x\cdot y)^2 + 4\cdot x\cdot y\cdot \sin^2\left(\frac{\phi}{2}\right)}\right]. \tag{2.24}$$

2.17.2 Double Coupler Ring Resonator Filter (DCRR)

Consider the architectures of double coupler ring resonator which sometime called add/drop filters as illustrated in Fig. 2.10, which are constructed by 2×2 optical couplers.

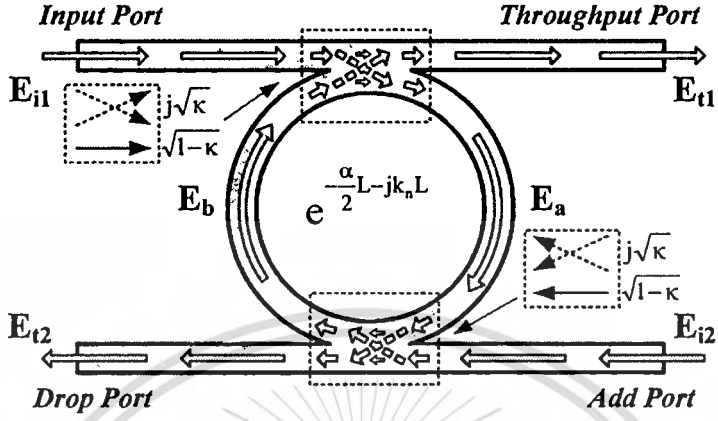

Fig. 2.10 The single ring resonator with two adjacent waveguides.

For simplification, the calculation of the intensity relation does not take into account coupling losses ($D^2 = 1$).

$$E_a = E_{i1} j\sqrt{\kappa_1} + E_b\sqrt{1-\kappa_1}\, e^{-\frac{\alpha L}{2\,2}-jk_n\frac{L}{2}} \tag{2.25}$$

$$E_b = E_a\sqrt{1-\kappa_2}\, e^{-\frac{\alpha L}{2\,2}-jk_n\frac{L}{2}} \tag{2.26}$$

$$E_a = \frac{E_{i1} j\sqrt{\kappa_1}}{1-\sqrt{1-\kappa_1}\sqrt{1-\kappa_2}\, e^{-\frac{\alpha}{2}L-jk_nL}} \tag{2.27}$$

$$E_b = \frac{E_{i1} j\sqrt{\kappa_1}}{1-\sqrt{1-\kappa_1}\sqrt{1-\kappa_2}\, e^{-\frac{\alpha}{2}L-jk_nL}} \cdot \sqrt{1-\kappa_2}\, e^{-\frac{\alpha L}{2\,2}-jk_n\frac{L}{2}} \tag{2.28}$$

$$E_{i1} = E_b\, j\sqrt{\kappa_1}\, e^{-\frac{\alpha L}{2\,2}-jk_n\frac{L}{2}} + E_{i1}\sqrt{1-\kappa_1} \tag{2.29}$$

$$E_{t2} = E_a\, j\sqrt{\kappa_2}\, e^{-\frac{\alpha L}{2\,2}-jk_n\frac{L}{2}} \quad \text{at } E_{i2} = 0 \tag{2.30}$$

Where E_{i1} is the input field, E_{t1} is the throughput field, E_{t2} is the dropped field, E_{t1}, E_a and E_b are the fields in the ring, κ_1 is thefield coupling coefficient between the input bus and the ring, κ_2 is the field coupling coefficient between the ring and the input bus, L is the circumference of the ring,

By using the upper equations, the transfer function for throughput port and drop port in Fig. 2.10 can thus be expressed as

Throughput port:

$$\frac{E_{t1}}{E_{i1}} = \frac{-\kappa_1\sqrt{1-\kappa_2}\, e^{-\frac{\alpha}{2}L-jk_nL} + \sqrt{1-\kappa_1} - (1-\kappa_1)\sqrt{1-\kappa_2}\, e^{-\frac{\alpha}{2}L-jk_nL}}{1-\sqrt{1-\kappa_1}\sqrt{1-\kappa_2}\, e^{-\frac{\alpha}{2}L-jk_nL}} \tag{2.31}$$

$$\frac{E_{t1}}{E_{i1}} = \frac{-\sqrt{1-\kappa_2}\, e^{-\frac{\alpha}{2}L-jk_nL} + \sqrt{1-\kappa_1}}{1-\sqrt{1-\kappa_1}\sqrt{1-\kappa_2}\, e^{-\frac{\alpha}{2}L-jk_nL}} \tag{2.32}$$

Drop port:

$$\frac{E_{t2}}{E_{i1}} = \frac{-\sqrt{\kappa_1\kappa_2}\, e^{-\frac{\alpha L}{2\,2}-jk_n\frac{L}{2}}}{1-\sqrt{1-\kappa_1}\sqrt{1-\kappa_2}\, e^{-\frac{\alpha}{2}L-jk_nL}} \tag{2.33}$$

The intensity relations for the throughput and drop port can be obtained by normalizing the transfer functions in Eqs. (2.34) and (2.35) which are given by

$$\frac{I_{t1}}{I_{i1}} = \left|\frac{E_{t1}}{E_{i1}}\right|^2 = \frac{1-\kappa_1-2\sqrt{1-\kappa_1}\sqrt{1-\kappa_2}\, e^{-\frac{\alpha}{2}L}\cos(k_nL) + (1-\kappa_2)e^{-\alpha L}}{1+(1-\kappa_1)(1-\kappa_2)e^{-\alpha L} - 2\sqrt{1-\kappa_1}\sqrt{1-\kappa_2}\, e^{-\frac{\alpha}{2}L}\cos(k_nL)} \tag{2.34}$$

$$\frac{I_{t2}}{I_{i1}} = \left|\frac{E_{t2}}{E_{i1}}\right|^2 = \frac{\kappa_1\kappa_2\, e^{-\frac{\alpha}{2}L}}{1+(1-\kappa_1)(1-\kappa_2)e^{-\alpha L} - 2\sqrt{1-\kappa_1}\sqrt{1-\kappa_2}\, e^{-\frac{\alpha}{2}L}\cos(k_nL)} \tag{2.35}$$

2.18 Optical Filters

A key element for controlling light in WDM systems is the optical filter. Here are mainly two classes of optical filters.

- Finite impulse response (FIR) or moving average (MA) filters : filters that do not rely on any feedback mechanism, i.e., do not rely on optical reflections. These filters are sometimes called feed-forward, such as Mach Zehnder based filters and waveguide grating routers (WGRs).

- Infinite impulse response (IIR) or autoregressive (AR) filters : filters inherently based on multiple reflections. Examples of these include fiber brag gratings (FBGs), thin film filters (TFFs), and optical all-pass filter (APFs).

The description of some of the most common optical filters [82] is given by:

2.18.1 Plane Grating

A typical reflective grating consists of a mirrored surface with tiny periodically located grooves. When illuminated, the light reflected from one groove interferes with the light reflected from other grooves, resulting in constructive and destructive interference. The wavelength dependence of the interference patterns are exploited to separate the different wavelengths which are detected for example by using a photodiode.

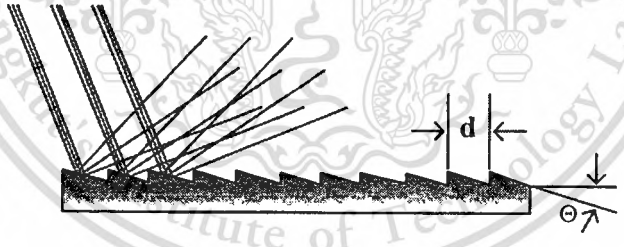

Fig. 2.11 Plane grating.

2.18.2 Fabry-Perot Interferometer

This principle of this filter was invented in 1898 by the French physicists Charles Fabry and Alfred Perot. The principle is still the same; two highly reflective parallel mirrors are separated by a small distance. Most of the light which encounters the first mirror is reflected, but some of it transmits, travel through the cavity (the space between the mirrors, often filled with some kind of dielectric e.g. liquid crystals (LCs)), and strikes the second mirror. At the second mirror most of the light is reflected, while some transmits.

The reflected light travels backwards, hitting the first mirror, where some of the again reflects and some transmits. The result is that depending on the spacing and index of refraction between the mirrors, at some wavelengths the multiple reflections interfere constructively. At these wavelengths the transmitted waves add out of phase and the reflected waves add in phase. At these wavelengths the interferometer's overall transmission is low, and the overall reflectivity is high.

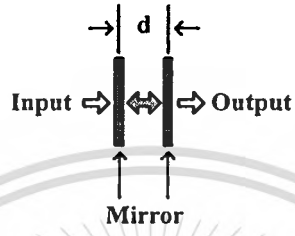

Fig. 2.12 Fabry-Perot Interferometer.

2.18.3 Fiber Bragg Grating [83]

These types of filters consist of a region in which the index of the fiber varies periodically between high and low, and they are formed in optical fibers by exposing the fiber to interferometric patterns from an ultraviolet (UV) laser. As in the Fabry-Perot interferometer, multiple reflected and transmitted waves result. For a specific wavelength the reflected waves all add in phase, and at this wavelength the grating appears to be highly reflective, while transmitting all the others.

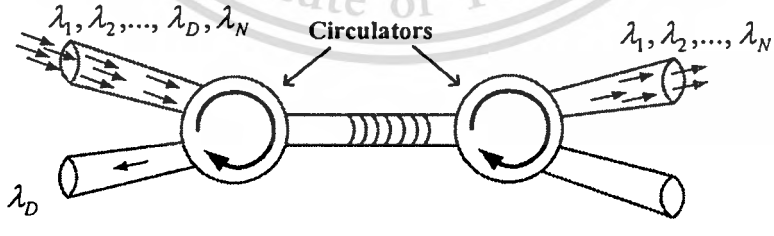

Fig. 2.13 Optical Fiber Bragg Grating.

2.18.4 Arrayed Waveguide Grating (AWG) [84]

The most common filter in optical telecommunications is this type of filter. The AWG uses an array of single mode waveguides in which the lengths of adjacent waveguides differ by a

fixed amount. The input light from a single fiber illuminates all these waveguides. Because of the different lengths of the waveguides, the phase of the light (at the output end of the array of waveguides) varies by a fixed amount, from one waveguide to the next. This variation results in a wavelength dependent phase front that is similar to the one from a plane grating. This pattern is then arranged so that different wavelengths illuminate different output fibers. The AWG can serve as a wavelength multiplexer as well as a demultiplexer.

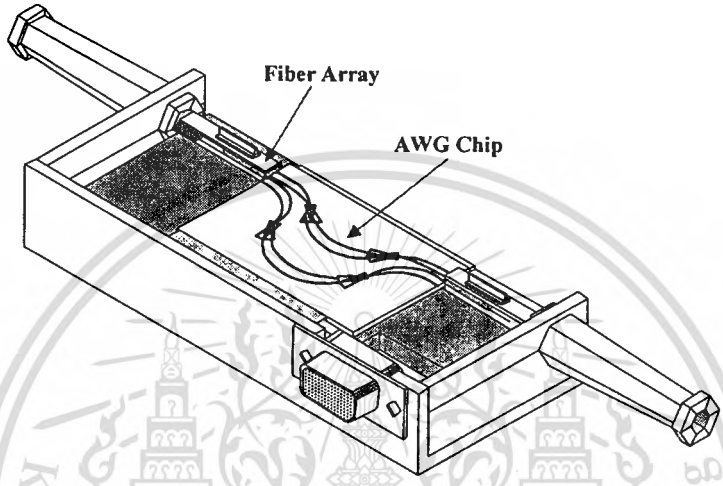

Fig. 2.14 Packaged arrayed waveguide grating.

2.18.5 Mach Zehnder Interferometer (MZI)

This filter consists of a pair of couplers connected by two paths of unequal length. Group velocity dispersion in the optical paths of different lengths results in some wavelengths being output to the top port, and other wavelengths being output to the bottom port.

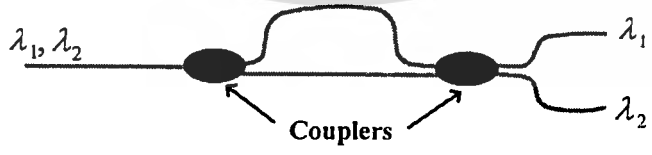

Fig. 2.15 Mach Zehnder Interferometer.

2.18.6 Thin Film Dielectric Interference Filter

This filter requires the deposition of many layers of coating to create narrow-band filters. A typical filter with a 3 dB bandwidth of 100 GHz requires more than a hundred layers of

coating. With so many layers being deposited, errors caused by local film thickness variation and alternation in density increase, reduce the yield of useful filters. A transmitted beam that goes through a filter is composed of multiple sub-beams, each having a slightly different travel time, which adds dispersion to the data signal.

2.19 Summary

This chapter introduces the nonlinear optics, the optical soliton which used as the input for launching into the optical devices and the principle concepts of different optical devices. Next, we use the concept in this chapter in design the devices in Chapter 3, 4, 5 and 6. In the next chapter, the optical and quantum security are introduced.

CHAPTER 3

CONTINUOUS VARIABLE QUANTUM KEY DISTRIBUTION

In this chapter, we introduce to the generation of polarized soliton pulses for multi links in the section 3.2 and 3.3. The continuous variable quantum key distribution is introduced in the section 3.4. The entangled photons are described in the section 3.5.

3.1 Introduction

Quantum security has shown the promising indication of the realistic application for perfect security, whereas the message (i.e. telephone conversation) in the classical channel could be multiplexed with the secure quantum codes (qubits). Some research works in several techniques have shown the potential of applications [85-87]. They have shown that the entangled photon pair can be used as the quantum bits, where the random entangled states can be used to generate the random codes (0 and 1). However, the problem of the system degradation due to walk-off effects [88, 89] and power loss in long distance link remains. Furthermore, the problem of polarization dispersion causes the entangled photon a problem which is called entangled state timing walk-off, which is become a problem in the recovery process. In practice, to solve such a problem, a technique called walk-off compensation and a quantum repeater are recommended to implement into the long distance link. To date, the searching of new device for mobile telephone hand set that capable to implement the said technology within the device is very attractive, i.e. quantum encoding. Fortunately, it seems that the scale of such a device (i.e. micro ring) is dramatically decreased, where the device scale of few microns is fabricated and available [90, 91]. One of the promising aspects is that such a device can be fabricated to process the signal processing within the small device, where the secured message, i.e. security, can be performed [92]. Some techniques such as chaos [93, 94], quantum entanglement [85] and chaotic quantum [95] have shown the potential of applications for communication security, however, the problem of signal taping and signal degradation remains in long distance link. Recently, Khunnan and Yupapin [96] have shown that the entangled photon recovery i.e. regeneration using fiber optic ring resonator incorporating an EDFA which is useful for long distance link. In this chapter, we

propose the system that can be implemented for secure long distance link. Firstly, the chaotic signals are generated by a soliton pulse within the micro ring resonators. Secondly, the quantum codes are generated by a micro ring device and a polarization control unit. The high power second harmonic pulses can be performed the strong entangled photon pair, which is capable for long distance link. Further, the multi entangled photon sources are also available, which also discussed in details. Finally, the continuous variable quantum key distribution is described.

3.2 Operating Principle

We are looking for a stationary soliton pulse, which is introduced into the multi-stage micro ring resonators as shown in Fig. 3.1, the input optical field (E_{in}) is given by [97]

$$E_{in} = A\,\mathrm{sech}\left[\frac{T}{T_0}\right]\exp\left[\left(\frac{z}{2L_D}\right) - i\omega_0 t\right] \tag{3.1}$$

Where A and z are the optical field amplitude and propagation distance, respectively. T is a soliton pulse propagation time in a frame moving at the group velocity, $T = t - \beta_1 \times z$, where β_1 and β_2 are the coefficients of the linear and second order terms of Taylor expansion of the propagation constant. $L_D = T_0^2/|\beta_2|$ is the dispersion length of the soliton pulse. The frequency shift of the soliton is ω_0. This solution describes a pulse that keeps its temporal width invariance as it propagates, and thus is called a temporal soliton. When a soliton peak intensity $\left(|\beta_2/\Gamma T_0^2|\right)$ is given, then T_0 is known. For the soliton pulse in the micro ring device, a balance should be achieved between the dispersion length (L_D) and the nonlinear length ($L_{NL} = 1/\Gamma\phi_{NL}$), where $\Gamma = n_2 \times k_0$, is the length scale over which dispersive or nonlinear effects makes the beam becomes wider or narrower. For a soliton pulse, there is a balance between dispersion and nonlinear lengths, hence $L_D = L_{NL}$.

When light propagates within the nonlinear material (medium), the refractive index (n) of light within the medium is given by

$$n = n_0 + n_2 I = n_0 + \left(\frac{n_2}{A_{eff}}\right)P, \tag{3.2}$$

Where n_0 and n_2 are the linear and nonlinear refractive indexes, respectively. I and P are the optical intensity and optical power, respectively. The effective mode core area of the device is given by A_{eff}. For the micro ring and nano ring resonators, the effective mode core areas range from 0.50 to 0.1 μm^2.

When a soliton pulse is input and propagated within a micro ring resonator as shown in Fig. 3.1, which consists of a series micro ring resonators. The resonant output is formed, thus, the normalized output of the light field is the ratio between the output and input fields ($E_{out}(t)$ and $E_{in}(t)$) in each roundtrip, which can be expressed as

$$\left|\frac{E_{out}(t)}{E_{in}(t)}\right|^2 = (1-\gamma)\left[1-\frac{(1-(1-\gamma)x^2)\kappa}{(1-x\sqrt{1-\gamma}\sqrt{1-\kappa})^2+4x\sqrt{1-\gamma}\sqrt{1-\kappa}\sin^2(\frac{\phi}{2})}\right] \tag{3.3}$$

The close form of equation (3.3) indicates that a ring resonator in the particular case is very similar to a Fabry-Perot cavity, which has an input and output mirror with a field reflectivity, $(1-\kappa)$, and a fully reflecting mirror. κ is the coupling coefficient, and $x = \exp(-\alpha L/2)$ represents a roundtrip loss coefficient, $\phi_0 = kLn_0$ and $\phi_{NL} = kLn_2|E_{in}|^2$ are the linear and nonlinear phase shifts, $k = 2\pi/\lambda$ is the wave propagation number in a vacuum. Where L and α are a waveguide length and linear absorption coefficient, respectively. In this work, the iterative method is introduced to obtain the results as shown in equation (3.3), similarly, when the output field is connected and input into the other ring resonators.

3.3 Polarized Soliton Pulses Generation for Multi Links

The remarkably simple system of the intense short pulse generation using a serial micro ring resonator is shown in Fig. 3.1. When a soliton pulse is input into the nonlinear Kerr effects medium, the nonlinear behavior of light traveling in a micro ring resonator is introduced. In principle, the clear second harmonic light mode is required in this technique, therefore, the chaotic signal is recommended to generate within the series micro ring resonators. After the soliton pulse is input into the first micro ring device as shown in Fig. 3.1, there are some light modes generated with smaller spectral with than the input pulse, which is obtained by the generated chaotic signals.

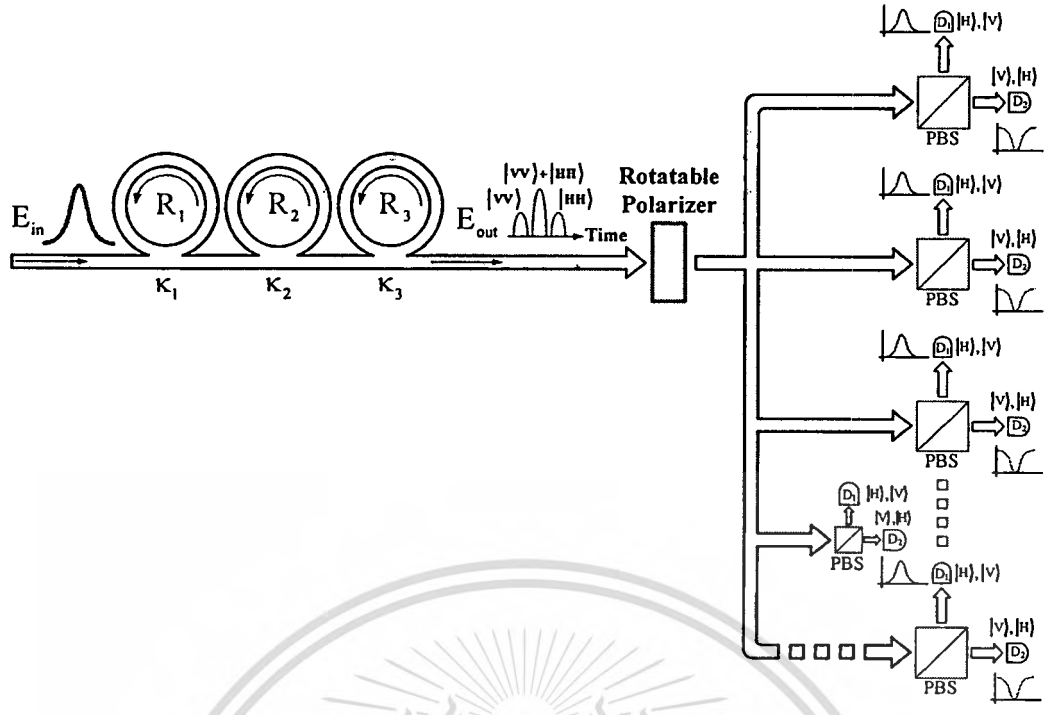

Fig. 3.1 Show a schematic diagram of the micro ring resonators of a continuous variable quantum key distribution with the different time slot entangled photon encoding for long distance link, where PBS is a polarizing beamsplitter and D_s are the avalanched detectors.

The selected wavelengths or modes at the specific wavelength are required to obtain the specific use. The optical filter characteristics is employed by using the appropriate ring parameters such as input power and wavelength, ring material refractive index, radius and coupling constant etc. In this investigation, the soliton input power is 450 mW, with centre wavelength at $\lambda_0 = 1.55$ μm, $n_0 = 3.34$, $n_2 = 2.2 \times 10^{-15}$ m^2W^{-1}, $A_{eff} = 0.25$ μm^2, $\alpha = 0.5$ $dBmm^{-1}$, $\gamma = 0.1$, roundtrips of 20,000. The wave guided loss used is 0.5 $dBmm^{-1}$. Fig. 3.2 shows the signal behaviors when light pulse is input into the series ring resonators. This can be made to design and select the specific output signal by using the appropriate ring radius and the coupling coefficient (κ). When the soliton input power of 450 mW, with pulse width of 50 fs is input into the first ring, the chaotic signal is generated. The clear second harmonic pulses are obtained by the last ring (R_3). Where the filtering chaotic signal is obtained with the lower and higher wavelengths at $\lambda_L = 775$ and $\lambda_H = 2{,}325$ nm, respectively. The centre wavelength is $\lambda_0 = 1.55$ μm. After the clear second harmonic pulses are combined via the PBS as shown in Fig. 3.1, the optimum entangled photon visibility is obtained as shown in Fig. 3.3. The remaining optical power is more than 80 % of the input power, which means that there is an amplified part

in the system. The soliton behavior is seen, which is suitable for long distance link, while the multi light sources used are also available.

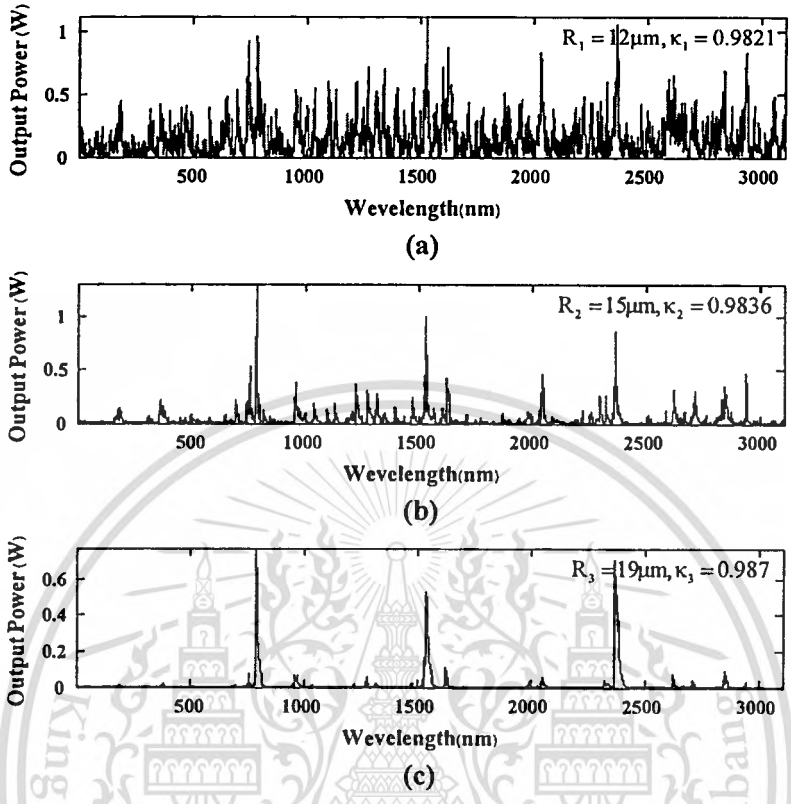

Fig. 3.2 Shows of the chaotic soliton generated by within micro ring resonators.

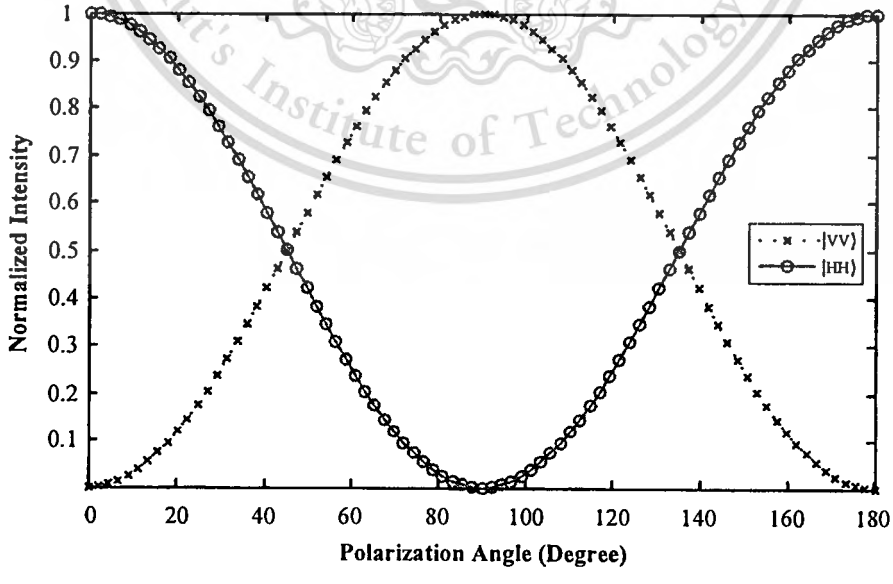

Fig. 3.3 Graph of the entangled photon visibility versus the polarization angle.

When polarized light propagates in optical ring device, the change in birefringence is introduced. This means the changed in phase of the entangled photon pair is occurred. Where the transversal walk-off produces a shift between the ordinary and extraordinary, while the longitudinal walk-off introduces a time delay between horizontally and vertically polarized photons. The amount of the walk-off depends on the location where the photon-pairs are created within the device. This position is completely random due to the coherent nature of light in the optical device. To compensate the longitudinal timing-walk off effect, a polarization controller is recommended to ensure that the polarization rotation is the same on both photons from the entangled pair. Additionally the compensator device is used to change the relative phase ϕ of the states of the polarized light. Because of the change in birefringence, the tilting of the compensator allows to apply a phase shift to the entangled states of the two entangled photons, which is given by Equation (3.4) as

$$|\psi\rangle_{12} = \frac{1}{\sqrt{2}}\left(|H\rangle_1 \otimes |V\rangle_2 + e^{i\phi}|V\rangle_1 \otimes |H\rangle_2\right) \tag{3.4}$$

In applications, the walk-off entangled state parameters involving in the measurement are related to the changes in the applied physical parameters such as force, stress, strain, heat, and pressure etc and the fiber optic properties. However, the interested parameters in this proposed systems are concerned the fiber optic birefringence parameters, which can be given by

$$\Delta\phi = \frac{2\pi(n_x - n_y)L_w}{\lambda} \tag{3.5}$$

Where $\Delta n = (n_x - n_y)$ is the fiber optic birefringence, L_w is the entangled states walk-off length, and λ is the light source wavelength.

However, the compensation can be made by using the related parameters as shown in Equation (3.5). The advantage of this system is that the quantum repeater can be redundant in long distance communication. In case of long distance link, the initial state is required to confirm the correct quantum codes between Alice and Bob, whereas the multi-users are also applicable respecting to the available link power in the transmission line.

3.4 Continuous Variable Quantum Key Distribution

The system of the continuous signals is as shown in Fig. 3.1 and 3.4. Firstly, to generate the continuous signals, i.e. spreading signals over the spectrum, which they are considered by the two concepts, i.e. the simultaneous frequency bands and the continuous entangled photon. The single mode soliton pulse is become many modes (noisy signals) after circulating within the first micro ring device due to the nonlinear Kerr effects of light within the micro ring resonator, which is called chaos. The advantageous of s soliton nonlinear property known as self phase modulation (SPM) introduces the signal spreading over the spectrum. The filtering characteristics of the signals within the ring devices are formed by choosing the appropriate ring parameters, especially, the coupling constants. However, in practice, the evidence of such a device in realistic application is required. By using the material parameters of InGaAsP/InP, the broad spectrum frequency bands can be obtained, finally, we end up with the following details. The soliton waveform with the center frequency at 2.0 GHz is input into the first micro ring resonator (R1). The optical power is fixed to 550 mW, $f_0 = 2.0$ GHz, $n_0 = 3.34$, $n_2 = 2.2 \times 10^{-17}$ m^2W^{-1}, $A_{eff} = 0.50$ μm^2, $\alpha = 0.5$ $dBmm^{-1}$, $\gamma = 0.1$, with 20,000 roundtrips. The chaotic signals are generated within the first ring (R_1), where the broad frequency band is observed in ring R_2. The clearer filtering signals are seen in ring R_3 and R_4. In Fig. 3.2, has shown that the spread frequency spectrum is generated within the micro ring R1, where the filtering signals are seen in the micro ring R_2, R_3 and R_4. The simultaneous frequency bands can be provided as shown in ring R_3, where the clearer signal is seen in ring R_4. The selected frequency bands in this case are 500 MHz and 2.0 GHz, which they have been commonly used in optical-wireless communication link. However, the other frequency bands can be performed by changing the ring parameters, which can be a broad spectrum, i.e. continuous spectrum.

Secondly, to generate the continuous variable entangled photons, the chaotic signal is recommended to employ within the series micro ring resonators. After the soliton pulse is input into the first micro ring device as shown in Fig. 3.1(a), the continuous light modes are generated, i.e. with narrower spectral width than the input pulse, which is obtained by the chaotic signal generation. This is allowed the selected wavelengths or modes at the specific wavelength to form the different time slot entangle photon pair. For instance, when the soliton input power is 450 mW, with centre wavelength at $\lambda_0 = 1.55$ μm, $n_0 = 3.34$, $n_2 = 2.2 \times 10^{-15}$ m^2W^{-1}, $A_{eff} = 0.25$ μm^2, $\alpha = 0.5$ $dBmm^{-1}$, $\gamma = 0.1$, roundtrips of 20,000. The wave guided loss used is 0.5 $dBmm^{-1}$. In Fig. 3.2, the continuous signal is generated within the ring R_1, where the filtering

signals are seen in rings R_2 and R_3 respectively. Results obtained have shown that this can be used to design and select the specific output signal by using the appropriate ring radii and the coupling coefficients (κ). When the soliton input power of 450 mW, with pulse width of 50 fs is input into the first ring, the chaotic signal is generated. The clear second harmonic pulses are obtained by the last ring (R_3). Where the filtering chaotic signal is obtained with the lower and higher wavelengths at λ_L = 775 nm and λ_H = 2,325 nm, respectively. The centre wavelength is λ_0 = 1.55 μm. After the clear second harmonic pulses are combined via the PBS as shown in Fig. 3.1, the optimum entangled photon visibility is obtained as shown in Fig. 3.3. In application, the continuous variable entangled photon is required to provide the continuous variable quantum key distribution, where the different time slot detection of the entangled photon pairs can be formed spreading over the spectrum. These can be encoded by Alice, where the retrieval codes can be performed by Bob.

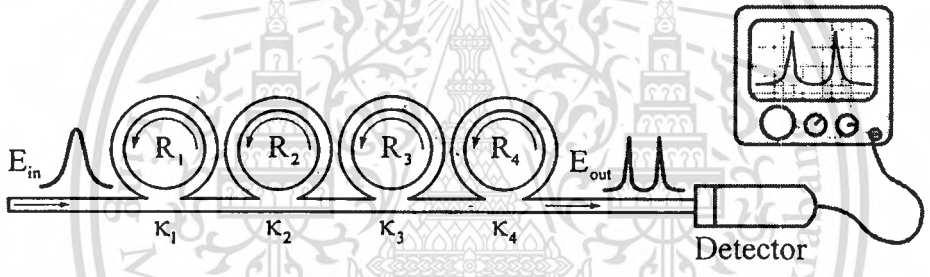

Fig. 3.4 A schematic diagram an up-down-link system, where R_S : ring radii, and κ_S : coupling coefficients.

In application, the simultaneous optical-wireless up-down-link system for continuous variable quantum key distribution is as shown in Fig. 3.4. The up-link system is performed by using the output from the throughput port which they are continuously generated. Similarly, the down link signals are continuously generated then input into the add port of the add/drop multiplexer. For examples, the up-link and down-link frequency bands are 2.0 GHz and 500 MHz, respectively, as shown in Fig. 3.5. However, in practice, the optical and electrical (E/O) converting device is required to form the up-down-link converters, where in some ways the coupling losses are introduced into the system. One pair of the second harmonic signals is shown in Fig. 3.2, where the output entangled photon pair can be formed by the polarization control unit. The initial quantum key is formed by Alice at a drop port. The required codes are retrieved by

Bob when the secret codes are given by Alice. In general, the quantum dense coding can be provided by using the continuous variable entangled photons, where each pair of the entangled photon is detected which is recognized by the time difference, i.e. different time slots. Furthermore, by using of the appropriate parameters, the signals can be trapped, i.e. stopped within the micro ring R_3. This means that the use of a quantum memory is plausible, which is the other interested work.

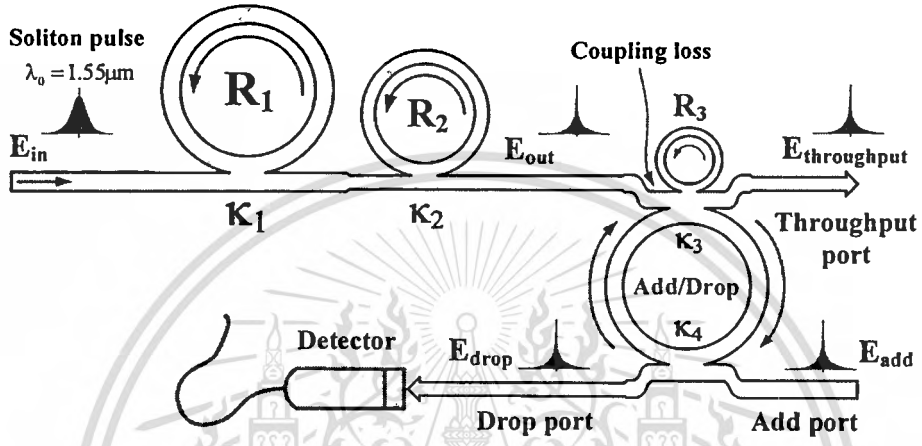

Fig. 3.5 A schematic of a combined system of a simultaneous optical-wireless up-down-link and a continuous variable quantum cryptography.

3.5. Entangled Photons

An excited atom emits two photons that come out back to back from the Einstein Podolsky Rosen (EPR) source [98], with vanishing angular momentum and even parity. If $|x\rangle$ and $|y\rangle$ are horizontal and vertical linear polarization states of the photon, then have seen that

$$|+\rangle = \frac{1}{\sqrt{2}}\left(|x\rangle + i|y\rangle\right)$$
$$|-\rangle = \frac{1}{\sqrt{2}}\left(i|x\rangle + |y\rangle\right) \tag{3.6}$$

are the eigenstates of helicity. For two photons, one propagating light is in the $+\hat{z}$ direction and other in the $-\hat{z}$ direction. The states

$$|+\rangle_A|-\rangle_B$$
$$|-\rangle_A|+\rangle_B \tag{3.7}$$

are invariant under rotations about $\hat{z}$. (The photons have opposite values of J_z, but the same helicity, since they are propagating in opposite directions.) Under a reflection in the y–z plane, the polarization states are modified according to

$$|x\rangle \to -|x\rangle \ , \ |+\rangle \to +i|-\rangle$$
$$|y\rangle \to |y\rangle \ , \ |-\rangle \to -i|+\rangle \tag{3.8}$$

Therefore, the parity eigenstates are entangled states

$$\frac{1}{\sqrt{2}}\left(|+\rangle_A|-\rangle_B \pm |-\rangle_A|+\rangle_B\right) \tag{3.9}$$

The state with $J_z = 0$ and even parity, then, expressed in terms of the linear polarization states, is

$$-\frac{i}{\sqrt{2}}\left(|+\rangle_A|-\rangle_B \pm |-\rangle_A|+\rangle_B\right) = \frac{1}{\sqrt{2}}\left(|xx\rangle_{AB} + |yy\rangle_{BA}\right)_n = |\phi^+\rangle_{AB} \tag{3.10}$$

Because of invariance under rotations about $\hat{z}$, the state has this form irrespective of how we orient the x and y axes. We can use a polarization of either photon along any axis in the xy plane. Let $|x(\theta)\rangle$, and $|y(\theta)\rangle$ denote the linear polarization eigenstates along axes rotated by angle θ relative to the canonical x and y-axes. We may define an operator as (the analog of $\vec{\sigma}.\hat{n}$)

$$\tau(\theta) = |x(\theta)\rangle\langle x(\theta)| - |y(\theta)\rangle\langle y(\theta)| \tag{3.11}$$

Which has these polarization states as eigenstate with respective eigenvalues as

$$|x(\theta)\rangle = \begin{pmatrix} \cos\theta \\ \sin\theta \end{pmatrix},$$
$$|y(\theta)\rangle = \begin{pmatrix} -\sin\theta \\ \cos\theta \end{pmatrix} \tag{3.12}$$

Let $|H\rangle$ and $|V\rangle$ be two polarization states of photon, which are sent from Alice to Bob along two separated channels. We shall take two orthogonal states $|\psi_+\rangle$ and $|\psi_-\rangle$, linear combinations of $|H\rangle$ and $|V\rangle$, to represent bit value "0" and bit value "1", respectively:

$$|\psi_+\rangle = \frac{1}{\sqrt{2}}(|H\rangle + |V\rangle) \tag{3.13}$$

$$|\psi_-\rangle = \frac{1}{\sqrt{2}}(|H\rangle - |V\rangle) \tag{3.14}$$

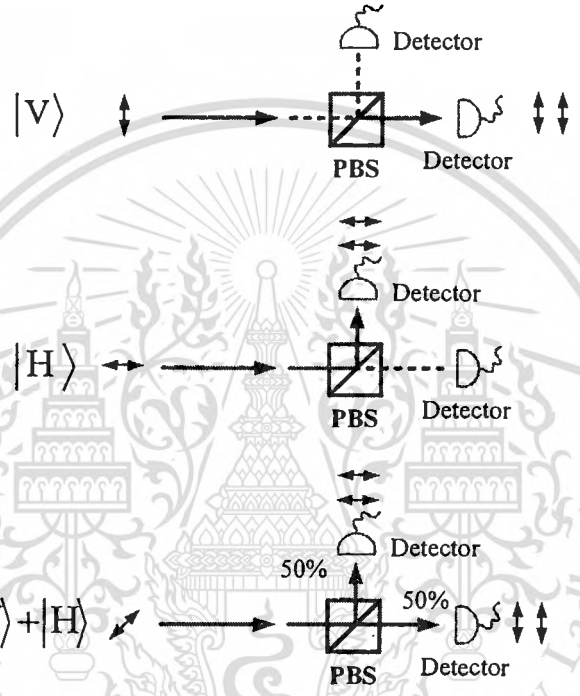

Fig. 3.6 Schematic diagram of a single photon entangled state.

Alice sends to Bob either $|\psi_+\rangle$ or $|\psi_-\rangle$. The two localized states, $|H\rangle$ and $|V\rangle$, are not sent together, but $|V\rangle$ is delayed for some time τ. For simplicity, we choose τ to be larger than the traveling time of the particles from Alice to Bob, θ. Thus $|V\rangle$ starts traveling towards Bob only when $|H\rangle$ already has reached Bob, such that the two wave packets and never found together in the transmission channels.

3.6 Summary

In chapter 3, we have proposed the technique of quantum soliton signals generated by a chaotic soliton pulse in micro ring resonators, whereas the high power second harmonic soliton pulses can be performed with the strong entangled photon visibility is proposed. The clear and strong entangled photons are generated using the proposed system, which is capable for multi and long distance links. However, a problem of quantum states cloning due to the very strong coupling power may be overcome, whereas the cloning protection from eavesdropper is our continuing work.

The very interesting concept where the continuous variable quantum key distribution can be performed via the simultaneous optical-wireless up-down-link system is proposed. The system is consisted of a series of nonlinear micro ring devices. We have shown that the two different frequency bands could be generated and selected, which they are normally used in the up-down-link converters in optical wireless link system. The key advantages of the system are the simultaneous generation of up and down link frequency bands, and the continuous frequency bands can be formed within the single system. The optical power in the system is generated by using a soliton pulse within the nonlinear Kerr type micro ring devices. Therefore, the remaining optical power is able to perform the link due to the soliton behavior. Further, there are more frequency bands available, which is suitable to implement more applications.

In next chapter, we will describe about communication security using quantum key distribution.

CHAPTER 4

COMMUNICATION SECURITY USING QUANTUM KEY DISTRIBUTION

In this chapter, a novel system of a simultaneous generation of continuous variable quantum key distribution (QKD) and quantum dense coding (QDC) via an optical memory array is proposed. The optical memory system is formed by using an array waveguide incorporating a nano ring resonator, whereas the different spatial light modes can be generated and stored within an optical memory unit. The polarized photon is formed and stored within a storing device, i.e. a ring resonator, whereas the different time slot entangled photons can be generated, transmitted and detected by the different subscriber in the distributed networks. By using the optical memory concept, the continuous variable quantum key distribution is provided. Furthermore, the use of quantum dense coding via time division multiplexing paths, i.e. different time slot, is also plausible. The advantage of the proposed system is that the quantum key distribution can provide the network top security with high capacity and safety, which is the large demand of usage in the public networks.

4.1 Introduction

Quantum key distribution (QKD) has been recognized as the top secret key for information security. It is only the method that can be used to keep the information in secret for communication and network security. Many research works have been proposed and investigated in both theoretical and experimental works, where several works have shown the promising results [91, 99-104] that can be used to make the realistic security, however, the searching of new technique and technology remains. Recently, Yupapin and Pornsuwancharoen [105] have reported the interesting result that light pulse can be stored within a nano-waveguide, which is available for quantum key generation source [104, 106-107]. Moreover, the continuous variable QKD can also be provided via the system. In this paper, we propose the concept of a quantum key generation via the optical memory within the array waveguide, which is available for a high capacity key generation called a parallel processing network distribution. In this concept, we assume that the quantum cryptography, i.e. quantum key and quantum code/decode can be

implemented by using the quantum keys via wireless or optical communication networks. Where each pair of the transmitted qubits can be randomly and continuously formed the output polarized photon by using each optical memory unit in the array. In this application, the idea of continuous QKD with QDC can be performed to create the more qubits with top security. Furthermore, such a design system can also be used with all types of network distributions, where the qubits can be performed and used in the link distributions.

4.2 Optical Memory Array

An optical memory unit is formed by using an optical waveguide structure as shown in Fig. 4.1 [105]. The upstream signal is generated by using a soliton pulse input into a ring resonator system, whereas it can be trapped (stored) within the memory device, i.e. a ring R4. The required signal with the selective wavelength can be filtered and trapped as shown in Fig. 4.1(b), the regeneration of the polarized photons can be performed via the downstream unit. By using the memory array as shown in Fig. 4.2, the dense wavelength multiplexing of the polarized photons can provide the higher capacity channel multiplexing, whereas the time division multiplexing photons is also available due to the different paths of incoming signals after combinations via the combiner. To begin this proposal, we introduce the technique that can be used to create the polarized entangle photon as shown in Fig. 4.3, a polarization coupler that separates the basic vertical and horizontal polarization states corresponds to an optical switch between the first and second incoming pulses. We assume those horizontally polarized pulses with a temporal separation of Δt. The coherence time of the consecutive pulses, i.e. between two pulses is larger than Δt. Then the following state is created by equation (4.1).

$$|\Phi\rangle_p = |1,H\rangle_s |1,H\rangle_i + |2,H\rangle_s |2,H\rangle_i \tag{4.1}$$

In the expression $|k,H\rangle, k$ is the number of time slots (1 or 2), where denotes the state of polarization, horizontal (H) or vertical (V), and the subscript identifies whether the state is the signal (s) or the idler (i) state. In Eq. (4.1), for simplicity we have omitted an amplitude term that is common to all product states. We employ the same simplification in subsequent equations in this paper. This two-photon state with H polarization shown by equation (4.1) is input into the orthogonal polarization-delay circuit shown schematically in Fig. 4.3. The delay circuit consists of a coupler and the difference between the round-trip times of the micro ring resonator, which is

equal to Δt. The micro ring is tilted by changing the round trip of the ring is converted into V at the delay circuit output. That is the delay circuits convert;

$$|k,H\rangle \text{ to } r|k,H\rangle + t_2 \exp(i\phi)|k+1,V\rangle + rt_2 \exp(i_2\phi)|k+2,H\rangle + r_2 t_2 \exp(i_3\phi)|k+3,V\rangle$$

Where t and r is the amplitude transmittances to cross and bar ports in a coupler. Then equation (4.1) is converted into the polarized state by the delay circuit as

$$\begin{aligned}
|\Phi\rangle &= [|1,H\rangle_s + \exp(i\phi_s)|2,V\rangle_s] \times [|1,H\rangle_i + \exp(i\phi_i)|2,V\rangle_i] \\
&\quad + [|2,H\rangle_s + \exp(i\phi_s)|3,V\rangle_s] \times [|2,H\rangle_i + \exp(i\phi_i)|2,V\rangle_i] \\
&= [|1,H\rangle_s|1,H\rangle_i + \exp(i\phi_i)|1,H\rangle_s|2,V\rangle_i] + \exp(i\phi_s)|2,V\rangle_s|1,H\rangle_i \\
&\quad + \exp[i(\phi_s+\phi_i)]|2,V\rangle_s|2,V\rangle_i + |2,H\rangle_s|2,H\rangle_i + \exp(i\phi_i)|2,H\rangle_s|3,V\rangle_i \\
&\quad + \exp(i\phi_s)|3,V\rangle_s|2,H\rangle_i + \exp[i(\phi_s+\phi_i)]|3,V\rangle_s|3,V\rangle_i
\end{aligned} \tag{4.2}$$

By the coincidence counts in the second time slot, we can extract the fourth and fifth terms. As a result, we can obtain the following polarization entangled state as

$$|\Phi\rangle = |2,H\rangle_s|2,H\rangle_i + \exp[i(\phi_s+\phi_i)]|2,V\rangle_s|2,V\rangle_i \tag{4.3}$$

We assume that the response time of the Kerr effect is much less than the cavity round-trip time. Because of the Kerr nonlinearity of the optical fiber, the strong pulses acquire an intensity dependent phase shift during propagation. The interference of light pulses at a coupler introduces the out put beam, which is entangled. Due to the polarization states of light pulses are changed and converted while circulating in the delay circuit, where the polarization entangled photon pairs can be generated. The entangled photons of the nonlinear ring resonator are separated to be the signal and idler photon probability. The polarization angle adjustment device as shown in Fig. 4.3 is applied to investigate the orientation and optical output intensity. In Fig. 4.3, we have proposed a system configuration that is made of an optical delay line incorporating micro ring resonator networks to code the optical pulse train and multiplexed with the coded pulse trains from other memory unit at a combiner. The system using delay line loops are very spectrally inefficient. A sub-picoseconds pulsed optical source having a pulse width much smaller than the bit duration is required. The entangled photons are formed by connecting the

polarization processing unit as shown in Fig. 4.3 to the Fig. 4.2 output, where the continuous variable and dense multiplexing photons can be projected and measured.

4.3 Simulation Result and Discussion

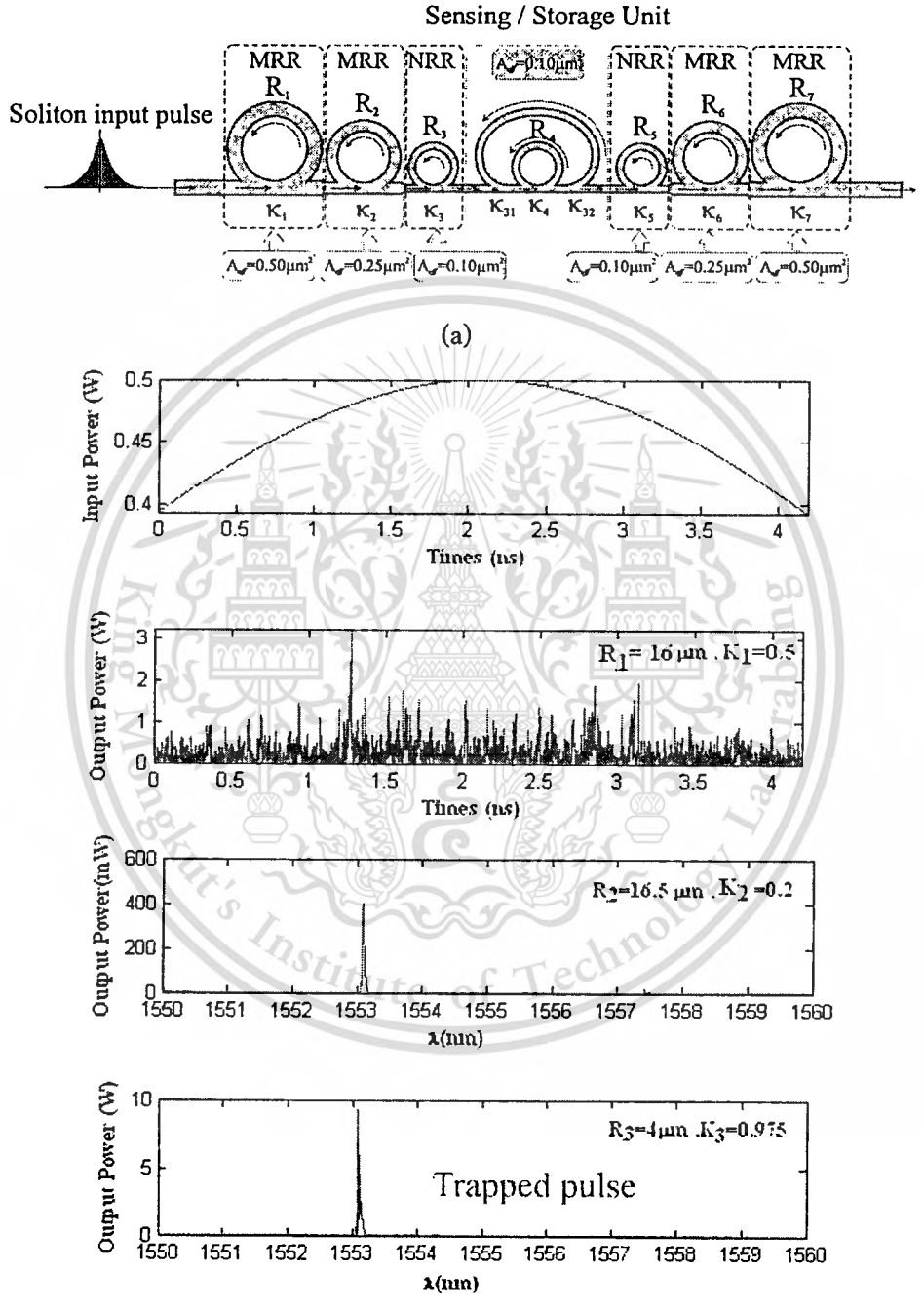

Fig. 4.1 An optical memory unit, where (a) a schematic of an upstream and downstream generation system with a storage unit, where R_s : ring radii, κ_s : coupling coefficients, MRR: micro ring resonator, NRR: nano ring resonator, (b) a trapped signal [105].

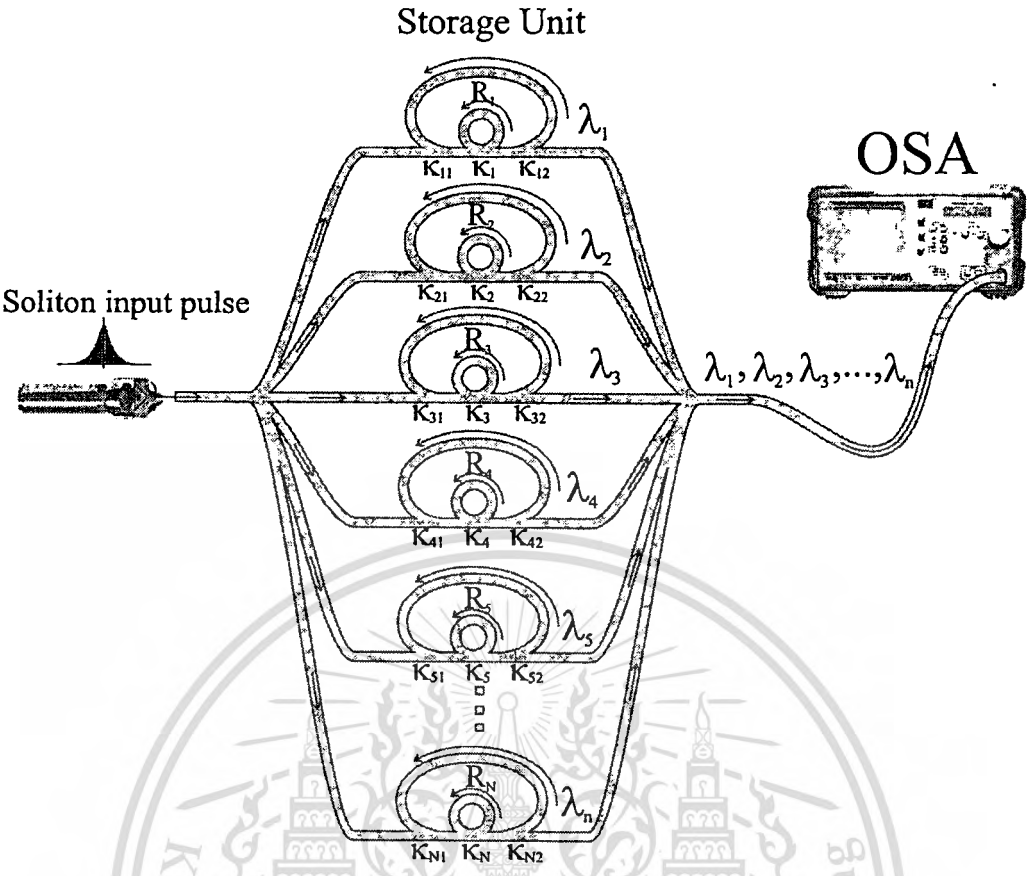

Fig. 4.2 Nano ring storage array waveguide system, where R_i : Ring radii, κ_i : Coupling coefficient, κ_{ij} : Coupling loss, λ_n : Signal output with wavelength λ_n , OSA : Optical Spectrum Analyzer.

Let us consider that the case when the signals from each memory unit is generated, where the reference photon passes through the path L ($2\pi R$) of a ring resonator as shown in Fig. 4.3, and it circulates within a micro ring resonator. In this case, the resonant photons reach the PBC at the same time. As in the parity checking described, the incoming photons in the states $|H\rangle_i|H\rangle_s$ and $|V\rangle_i|V\rangle_s$, where the two photons have different polarizations just before the PBC, which results in a two-photon state and the vacuum in the mode X, respectively. On the other hand, the photons in the state $\alpha|V\rangle_i|H\rangle_s + \beta|H\rangle_i|V\rangle_s$, which means that the two photons have the same polarization just before the PBC, which results in one photon in the mode X and one photon in Y, in the state $\alpha|H\rangle_X|H\rangle_Y + \beta|V\rangle_X|V\rangle_Y$. Hence, by counting the number of photons in the mode X, we can discard the cases $|H\rangle_i|H\rangle_s$ and $|V\rangle_i|V\rangle_s$. If Bob detects a photon in $|D\rangle_X$, the two photons are projected onto the state $|D\rangle_X(\alpha|H\rangle_Y + \beta|V\rangle_Y)$. Then Bob obtains the photon in the signal state $\alpha|H\rangle_Y + \beta|V\rangle_Y$.

In practical distributed network, photons in mode Y may be measured on a polarization basis. In this case, one can post-select the event where at least one photon is emitted in each mode X and Y by the two fold coincidence detection. Therefore, the conventional threshold photon detectors which do not discriminate two or more photons from the incident photons, can be used. In the other cases where the reference photon passes through the path S (incoming photon) and/or the signal photon passes through the path L(circulated photon), at least one of the photons should have a different arrival time at detector $|D\rangle_X$ or $|D\rangle_Y$. Hence we can eliminate the contributions from such cases by discriminating the arrival times of the photons at the detectors $|D\rangle_X$ and $|D\rangle_Y$ by post-selection, where the different time slot entangled photon can be distinguished and measured. Any loss in the channels and inefficiency of the detectors are also discarded by the post-selection. A single photon is formed in a ring resonator, which is obtained by the normalized entangled photons. Each of the entangled photon pair, which can be clarified by a quantum key between Alice and Bob, where the required memory and speed (time division multiplexed signals) are realized, can form the correct code, i.e. form the signal. In this application, the idea of the proposed optical encryption technique can be realized to form the QKD with QDC for top security in the distributed networks.

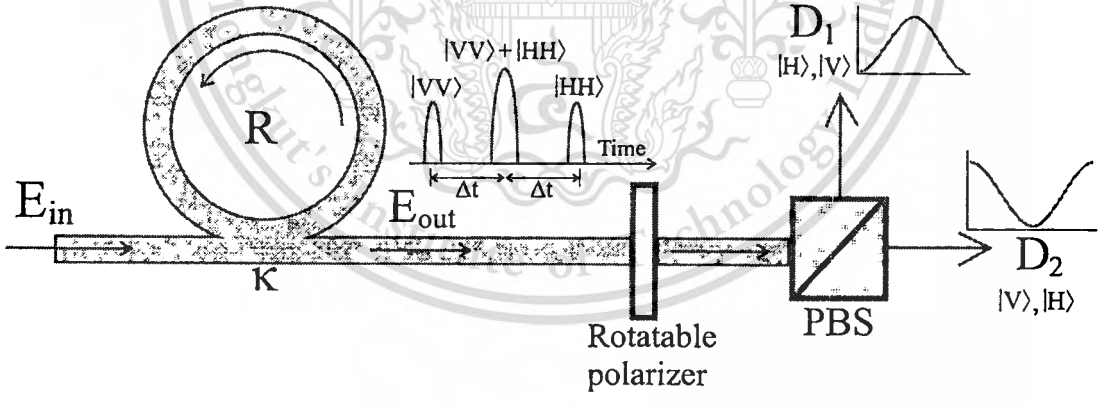

Fig. 4.3 A schematic of the entangled photon generation system; **PBS**: Polarizing Beam Splitter, D_S: Detectors.

4.4 Summary

We have proposed an interesting proposal of a continuous variable quantum key distribution and quantum dense coding system using an optical array waveguide, where the perfect security of communication information can be realized via an optical or wireless communication link. In practice, the set of all possible states is sent by Alice to Bob, whereas it is a set of two states corresponding to identical bits, where the two states are horizontal (H) and vertical (V) polarization photons instead of a photon, which is observed as a random orientation. The secret key is given to Bob (i.e. subscriber), where the required information can be retrieved by the specific subscribers in the network. In this application, the idea of the proposed optical/quantum encryption technique using the entangled photon pair can be implemented into the distributed networks. It can provide the secret key to create the top security for the large demand in the public networks.

CHAPTER 5

COMMUNICATION SECURITY USING DARK-BRIGHT SOLITON CONVERSION

In this chapter, we propose a novel scheme of communication security using a dark-bright soliton conversion behaviors, in which the transmission signals can be secured by the using the random codes generated by dark-bright soliton conversion within the system. The system consists of two parts, where firstly, an optical Mach Zhender interferometer (MZI) is used to generate the coincidence dark and bright soliton pair by using the $(\pi/2)$ phase retarder (i.e. a coupler), in which $|D\rangle$ and $|B\rangle$ states represent the orthogonal dark and bright soliton pulses. The signals from through (Th) port are formed and transmitted via the transmission line to the end user. Secondly, the add/drop filter is used to separate (filter) the required signal form the transmission link, in which the Th and drop port signals are formed as a reference and signal, respectively. In this case, we assume that both solitons are input into the MZI ports simultaneously (coincidently), in which the binary codes are randomly formed and used to present the transmission data, in which the state "0" and "1" are represented by $|DB\rangle$ and $|BD\rangle$, respectively. Finally, the eavesdropper and the signal accuracy are also described.

5.1 Introduction

Communication has become the important media and role in human daily life [108], in which the required communications in both wire and wireless communications [109, 110] must be fast and high security, therefore, the searching for new communication schemes still remains. Till date, many research works have been continuingly developed to increase in both speed and high security [111-113]. Lately, one of the interesting behaviors is that the use of dark-bright soliton conversion within the micro ring device has been proposed [114-117]. By using the dark-bright soliton pair, the random output of both solitons can be randomly interpreted and separated. The novel concept is that after the dark-bright soliton pair propagated through a $(\pi/2)$ phase retarder, the lack in phase of the coincident dark and bright solitons can be randomly separated and observed. In this work, a proposal of communication security using dark-bright soliton conversion is presented with interesting results. Firstly, the dark-bright soliton pair can be generated in a Mach

Zhender interferometer (MZI), in which the coincident dark and bright soliton pulses are propagated through a phase retarder, for instance, an optical coupler or a beam splitter. The simulation results were generated and obtained by the commercial MATLAB 2008b. From the obtained results, the dark and bright solitons are the orthogonal pulses and can be recognized as an entangled photon pair that can be used to form the random code for information security application. In operation, the MZI transmits the coincident dark and bright solitons into the transmission line to the end user, via the add/drop filter. The coincident dark and bright solitons are randomly separated at the output ports (Th and Drop ports) of the add/drop filter, respectively, in which the through and drop port signals can form the secure codes by the random appearance. By using the accuracy checking between sender and end user, the confirmation of the required information can be realized and the required information retrieved.

5.2 Dark-Bright Soliton Conversion in a MZI System

Dark and bright solitons are the short optical pulses that can propagate into the optical medium for long period of time due to their nonlinear properties, for instance, self phase and cross phase modulations [42]. The lack of phase with ($\pi/2$) between dark and bright solitons can be used to form the orthogonal photon components (entangled photon). More details of dark and bright soliton generation and behaviors can be found in both theory and experiment in the references [118-120]. Here, the proposed model for dark-bright soliton conversion based on MZI is as shown in Fig. 5.1. The output signals can be generated by dark-bright optical soliton conversion within the system, in which the dark soliton pulse $|D\rangle$ and the bright soliton pulse $|B\rangle$ are encoded into MZI. The random states between dark and bright solitons can be established, whereas the output of the orthogonal states can be randomly detected via the MZI output ports, which is the add/drop filter ports in this proposal. The reference, input and output signals in this operation are as shown in Figs. 5.1 and 5.2. In practice, the more random soliton states give more benefit to communication security requirement, in which the detection of one state is implied to the other state.

When the dark and bright soliton pulses are generated and input into the MZI, the optical fields propagating through the system are expressed by

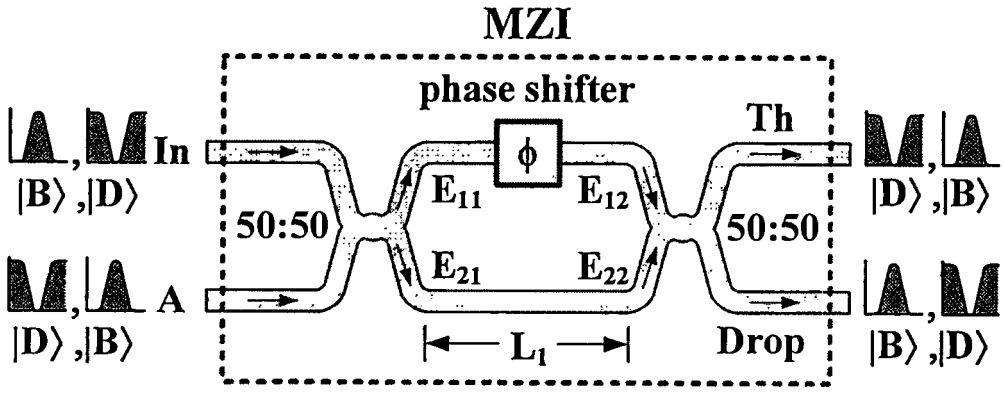

Fig 5.1 A schematic of dark and bright solitons conversion based on MZI.

$$E_{11} = \frac{1}{2}\mathrm{In} + j\frac{1}{2}A,$$
$$E_{21} = \frac{1}{2}A + j\frac{1}{2}\mathrm{In}, \tag{5.1}$$
$$E_{12} = E_{11}e^{-j\phi},$$
$$E_{22} = E_{21}e^{-\frac{\alpha}{2}L_1}, \tag{5.2}$$
$$\mathrm{Th} = \frac{1}{2}E_{12} + j\frac{1}{2}E_{22},$$
$$\mathrm{Drop} = \frac{1}{2}E_{22} + j\frac{1}{2}E_{12}, \tag{5.3}$$

where In is an input field, A is an added field (control), E_{11} and E_{21} are fields split into two arms of MZI passing through the first coupler as shown in Fig. 5.1. E_{12} and E_{22} are optical fields before merging into the second coupler. Th and Drop are the output field signals. L_1 is a lower MZI arm, with length of 8μm in this case. ϕ is the nonlinear phase shift depending on In and A input signals, and j is a complex conjugate term.

In simulation, the stationary dark and bright soliton pulses are introduced into the MZI ports as shown in Fig. 5.1. The input optical fields, E_{in} and E_{add}, of the dark and bright solitons, respectively, are given by [42, 118-120]

$$E_{in}(t) = A\tanh\left[\frac{T}{T_0}\right]\exp\left[\left(\frac{z}{2L_D}\right) - j\omega_0 t\right],$$
$$E_{add}(t) = A\,\mathrm{sech}\left[\frac{T}{T_0}\right]\exp\left[\left(\frac{z}{2L_D}\right) - j\omega_0 t\right], \tag{5.4}$$

where A and z are the optical field amplitude and propagation distance, respectively. T is a soliton pulse propagation time in a frame moving at the group velocity, $T = t - \beta_1 z$, where β_1 and β_2 are the coefficients of the linear and second-order terms of Taylor expansion of the propagation constant. $L_D = T_0^2/|\beta_2|$ is the dispersion length of the soliton pulse. T_0 in equation is a soliton pulse propagation time at initial input (or soliton pulse width), where t is the soliton phase shift time, and the frequency shift of the soliton is ω_0. This solution describes a pulse that keeps its temporal width invariance as it propagates, and thus is called a temporal soliton. When a soliton peak intensity ($\beta_2/\Gamma T_0^2$) is given, then T_0 is known. For the soliton pulse in the MZI device, a balance should be achieved between the dispersion length (L_D) and the nonlinear length ($L_{NL} = 1/\Gamma\phi_{NL}$), where $\Gamma = n_2 k_0$, is the length scale over which dispersive or nonlinear effects makes the beam become wider or narrower. For a soliton pulse, there is a balance between dispersion and nonlinear lengths, hence $L_D = L_{NL}$.

In operation, the dark-bright soliton conversion using a ring resonator optical channel dropping filter (OCDF) is composed of two sets of coupled waveguides, as shown in Fig. 5.2. The relative phase of the two output light signals after coupling into the optical coupler is $\pi/2$ before coupling into the ring and the input bus, respectively. This means that the signals coupled into the drop and through ports are acquired a phase of π with respect to the input port signal. In application, we can design and use the coupling coefficients appropriately, the field coupled into the through port on resonance would completely extinguish the resonant wavelength, and all power would be coupled into the drop port. The dark and bright soliton pulses propagate through the system, which they are expressed by

$$E_{ra} = -j\kappa_1 E_i + \tau_1 E_{rd}, \tag{5.5}$$

$$E_{rb} = \exp(j\omega T/2)\exp(-\alpha L/4)E_{ra}, \tag{5.6}$$

$$E_{rc} = \tau_2 E_{rb} - j\kappa_2 E_a, \tag{5.7}$$

$$E_{rd} = \exp(j\omega T/2)\exp(-\alpha L/4)E_{rc}, \tag{5.8}$$

$$E_t = \tau_1 E_i - j\kappa_1 E_{rd}, \tag{5.9}$$

$$E_d = \tau_2 E_a - j\kappa_2 E_{rb}, \tag{5.10}$$

where E_i is the input field, E_a is the add(control) field, E_t is the through field, E_d is the drop field, $E_{ra}...E_{rd}$ are the fields in the ring at points a...d, κ_1 is the field coupling coefficient between the input bus and ring, κ_2 is the field coupling coefficient between the ring

and output bus, L is the circumference of the ring, T is the time taken for one round trip (roundtrip time), and α is the power loss in the ring per unit length. We assume that this is the lossless coupling, i.e., $\tau_{1,2} = \sqrt{1-\kappa_{1,2}^2}$. $T = Ln_{eff}/c$.

The output power/intensities at the drop and through ports are given by

$$|E_d|^2 = \left| \frac{-\kappa_1\kappa_2 A_{1/2}\Phi_{1/2}}{1-\tau_1\tau_2 A\Phi} E_i + \frac{\tau_2 - \tau_1 A\Phi}{1-\tau_1\tau_2 A\Phi} E_a \right|^2, \quad (5.11)$$

$$|E_t|^2 = \left| \frac{\tau_2 - \tau_1 A\Phi}{1-\tau_1\tau_2 A\Phi} E_i + \frac{-\kappa_1\kappa_2 A_{1/2}\Phi_{1/2}}{1-\tau_1\tau_2 A\Phi} E_a \right|^2, \quad (5.12)$$

where $A_{1/2} = \exp(-\alpha L/4)$ (the half-round-trip amplitude), $A = A_{1/2}^2$, $\Phi_{1/2} = \exp(j\omega T/2)$ (the half-round-trip phase contribution), and $\Phi = \Phi_{1/2}^2$.

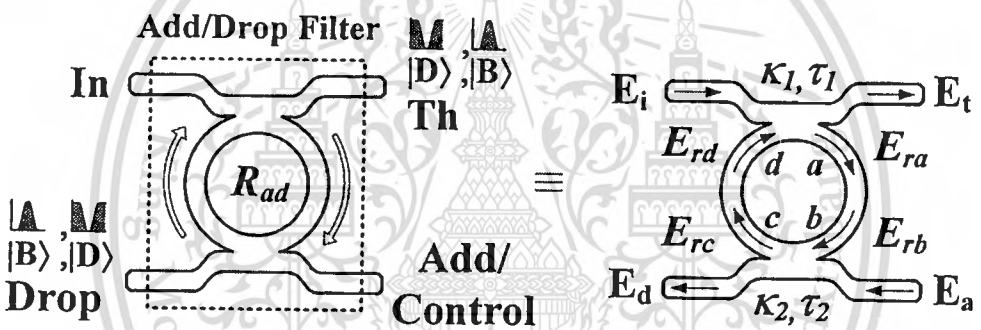

Fig 5.2 A schematic diagram of the Add/Drop Filter.

5.3 Security Proposal

In this simulation, the dark and bright soliton with the center wavelength at 1.55 μm are propagated into the MZI input ports. The attenuated soliton peak power at the input coupler is 1 W, 20 ns pulse width, and the waveguide loss of $1 dBmm^{-1}$ is included in the system (simulation). The input field of dark soliton $|D\rangle$ or bright soliton $|B\rangle$ is input into the MZI inputs (In and A ports), the input fields are combined and split into two parts with the same amount via a 3dB coupler (50:50), which they are E_{11} and E_{21}. The field E_{12} is the output field of E_{11} after propagating into the controlled phase shifted device, for instance, an optical coupler or a beamsplitter. Finally, the fields are combined again at the second 3dB coupler after the phase

controlled device, in which the random combination of the orthogonal pulses (dark and bright soliton pulses) can be obtained via the MZI ports.

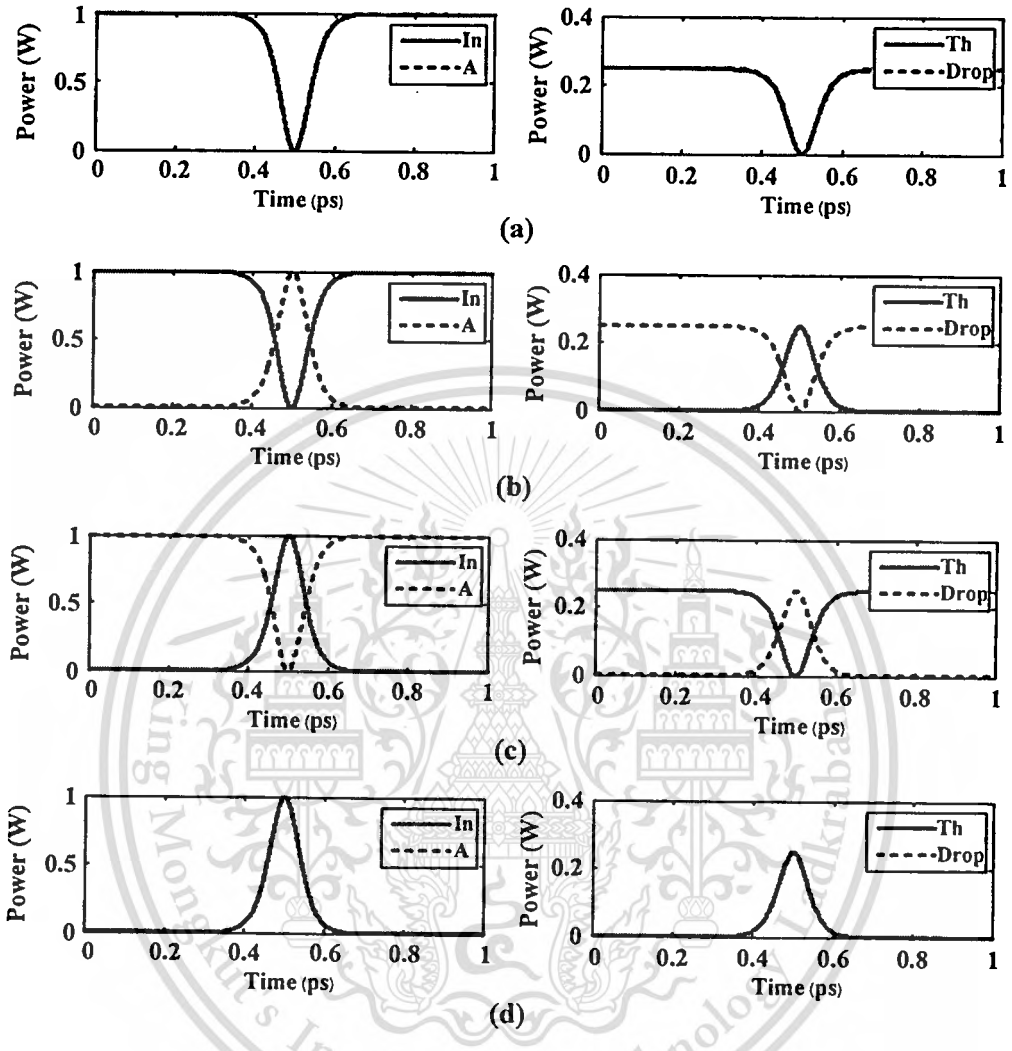

Fig 5.3 Simulation result of dark-bright soliton conversion when the logic inputs are (a) $|DD\rangle$, (b) $|DB\rangle$, (c) $|BD\rangle$, and (d) $|BB\rangle$.

When the dark-bright soliton pulses are input into MZI inputs, the obtained dark-bright soliton conversion at MZI outputs (Th and Drop ports) are $|DD\rangle \rightarrow |DD\rangle$, $|DB\rangle \rightarrow |BD\rangle$, $|BD\rangle \rightarrow |DB\rangle$ and $|BB\rangle \rightarrow |BB\rangle$, as shown in Fig. 5.3(a)-(d), respectively, in which the $|DB\rangle$ and $|BD\rangle$ are used instead of "0" and "1", respectively. The proposed system consists of two parts, which is schematically shown in Fig. 5.4. The first part is a MZI, which forms as a transmitter, whereas the dark-bright soliton pair is generated. The second part is a receiver, which is formed by the add/drop filter. In operation, a continuous optical dark-bright soliton pulses with

a wavelength of λ (1.55 μm) are input into the system via the input ports, which they are the In and A ports, respectively. The dark soliton $|D\rangle$ and bright soliton $|B\rangle$ are formed at the MZI output (Th and Drop port) as shown in Fig. 5.3. The end user receives the signal that transmits from the Th port, where the Drop port signal is used to form the referencing or monitoring signal. The accuracy checking can be applied for a high capacity transmission, where in this concept, the signal strength is used to consider for eavesdropping, for instance, if the signal strength is less than the required signal target limitation (for example 95 percent) then it will be considered as an eavesdropper, in which the signal data can be changed to avoid the cloning (copying) information, where the new code will be generated and used for the new transmission.

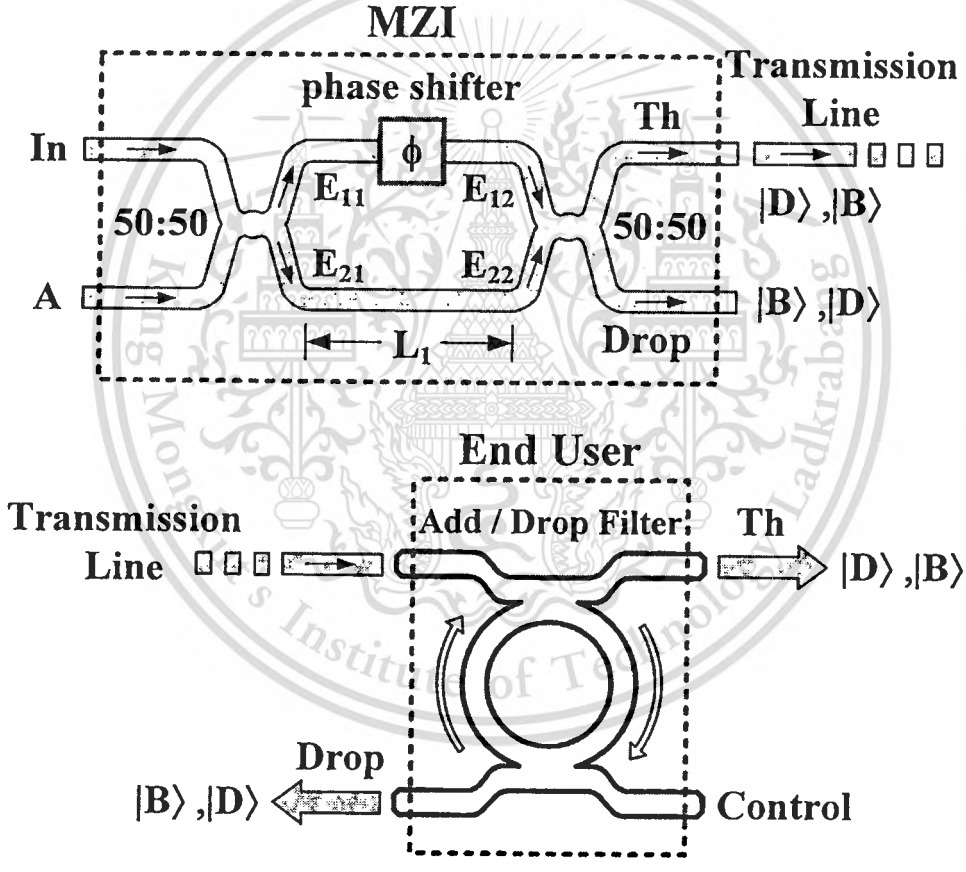

Fig 5.4 A schematic of communication security using dark-bright soliton conversion.

5.4 Summary

We have proposed an interesting concept of communication security using dark-bright soliton conversion within the MZI system, in which the randomly generated dark-bright soliton pair can be used to form the security codes, where finally, the accuracy checking of the final

codes can be performed between the end user and sender. By using soliton communication, the high strength signals can be obtained and realized for long distance communication. By considering the mathematic formulas of dark-bright soliton pair, the change in phase of them is formed by the orthogonal functions, which will be benefit to random coding and security requirement. Moreover, due to the lack of phase of $(\pi/2)$ between dark and bright solitons, which means that the use of such behaviors can form in the same way as the entangled photon behaviors, in which the use of dark-bright soliton pair for quantum information applications can be realized, which will be our continuing work.

CHAPTER 6

CONCLUSIONS

6.1 Conclusions

Two systems of an all optical system that can be used for optical communication security are proposed. Firstly, we have presented a system of a simultaneous generation of continuous variable quantum key distribution (QKD) and quantum dense coding (QDC) via an optical memory array is proposed. The optical memory system is formed by using an array waveguide incorporating a nano ring resonator, whereas the different spatial light modes can be generated and stored within an optical memory unit. The polarized photon is formed and stored within a storing device, i.e. a ring resonator, whereas the different time slot entangled photons can be generated, transmitted and detected by the different subscriber in the distributed networks. By using the optical memory concept, the continuous variable quantum key distribution is provided. Furthermore, the use of quantum dense coding via time division multiplexing paths, i.e. different time slot, is also plausible. The advantage of the proposed system is that the quantum key distribution can provide the network top security with high capacity and safety, which is the large demand of usage in the public networks. Finally, we propose a novel scheme of communication security using a dark-bright soliton conversion behaviors, in which the transmission signals can be secured by the using the random codes generated by dark-bright soliton conversion within the system. The system consists of two parts, where firstly, an optical Mach Zhender interferometer (MZI) is used to generate the coincidence dark and bright soliton pair by using the $(\pi/2)$ phase retarder (i.e. a coupler), in which $|D\rangle$ and $|B\rangle$ states represent the orthogonal dark and bright soliton pulses. The signals from through (Th) port are formed and transmitted via the transmission line to the end user. Secondly, the add/drop filter is used to separate (filter) the required signal form the transmission link, in which the Th and drop port signals are formed as a reference and signal, respectively. In this case, we assume that both solitons are input into the MZI ports simultaneously (coincidently), in which the binary codes are randomly formed and used to present the transmission data, in which the state "0" and "1" are represented by $|DB\rangle$ and $|BD\rangle$, respectively.

6.2 Future Works

Demand of using communication and internet has been increased widely and rapidly every year, therefore, the security of communication becomes the important function which is required to include into the modern device or internet service. To date, a quantum technique is recommended to provide such a requirement. However, the security technique known as quantum cryptography has been widely used and investigated in many applications. In future works, we will use a nonlinear micro ring resonator to form correlated photons and quantum codes, where the secret key codes can be generated by using the entangled photon pair, which can be formed by the secret key for two parties known as Alice and Bob by using the Gaussian light pulse propagating with the series of micro ring resonator. In application, the device can be embedded within the computer processing unit with using to increase the capacity and the speed for communication and internet, where the security of communication can be provided.

REFERENCES

[1] G. Keiser, **"Optical fiber communications 3rd Ed."** Boston: McGraw-Hill Inc, 1999.

[2] Y. Pei, Y. C. Liang, L. Zhang, K. C. Teh, and K. H. Li, "Secure communication over MISO cognitive radio channels," **IEEE Trans. Wireless Comm.**, vol. 9, no. 4, April 2010, pp. 1494-1502.

[3] M. Mimuro, S. Yamauchi, K. Suzuki, and Y. Imai, "Proposal for nonlinear refractive index measurement using spectral ratio in modulated OFRR dynamics," **Opt. Comm.**, vol. 281, no. 3, February 2008, pp. 469-473.

[4] X. Y. Wang and Y. F. Gao, "A switch-modulated method for chaos digital secure communication based on user-defined protocol," **Comm. Nonlin. Sci. and Numer. Sim.**, vol. 15, no. 1, 2010, pp. 99-104.

[5] X. M. Xiu, H. K. Dong, L. Dong, Y. J. Gao, and F. Chi, "Deterministic secure quantum communication using four-particle genuine entangled state and entanglement swapping," **Optics Comm.**, vol. 282, no. 12, June 2009, pp. 2457-2459.

[6] L. Dong, X. M. Xiu, Y. J. Gao, and F. Chi, "Deterministic secure quantum communication against collective-dephasing noise by using EPR pairs and auxiliary photons," **Optics Comm.**, vol. 282, no. 8, 2009, pp. 1688-1690.

[7] Y. S. Kivshar and B. Luther-Davies, "Dark optical solitons: physics and applications," **Phys. Rep.**, vol. 298, 1998, pp. 81-197.

[8] W. Zhao and E. Bourkoff, "Propagation properties of dark solitons," **Opt. Lett.**, vol. 14, no. 13, 1989, pp. 703–705.

[9] N. Pornsuwanchroen, S. Chaiyasoonthorn, and P. P. Yupapin, "Fast and slow lights generation using chaotic signals in the nonlinear micro ring resonators for communication security," **Opt. Eng.**, vol. 48, Jan 2009, p. 015002.

[10] N. Q. Ngo, "Proposal for a high-speed optical dark-soliton detector using a microring resonator," **IEEE Photon. Technol. Lett.**, vol. 19, no. 7, April 2007, pp. 471-473.

[11] I. V. Barashenkov, "Stability criterion for dark soliton," **Phys. Rev. Lett.**, vol. 77. 1996, p. 1193.

[12] D. N. Christodoulides, T. H. Coskun, M. Mitchell, Z. Chen, and M. Segev, "Theory of incoherent dark solitons," **Phys. Rev. Lett.**, vol. 80, 1998, p. 5113.

[13] M. Nakazawa, H. Kubota, K. Suzuki, E. Yamada, and A. Sahara, "Ultrahigh-speed long-distance TDM and WDM soliton transmission technologies," **IEEE J. Sel. Top. Quantum Electron.**, vol. 6 , 2000, p. 363.

[14] W. Zhao and E. Bourkoff, "Propagation properties of dark solitons," **Opt. Lett.**, vol. 14, 1989, p. 703.

[15] A. D. Kim, W. L. Kath, and C. G. Goedde, "Stabilizing dark solitons by periodic phase-sensitive amplification," **Opt. Lett.**, vol. 21, 1996, p. 465.

[16] B. A. Malomed, A. Mostofi, and P. L. Chu, "Transformation of a dark soliton into a bright pulse," **J. Opt. Soc. Am. B**, vol. 17, 2000, p. 507.

[17] P. P. Yupapin and W. Suwancharoen, "Chaotic signal generation and cancellation using a micro ring resonator incorporating an optical add/drop multiplexer," **Opt. Commun.**, vol. 280, 2007, p. 343.

[18] T. Zhang, X. F. Mo, Z. F. Han, and G. C. Guo, "Extensible router for a quantum key distribution network," **Phys. Lett. A**, vol. 372, 2008, p. 3957.

[19] B. S. Ham, "A novel method of all-optical switching: quantum router," **ETRI J.**, vol. 23, 2001, p. 106.

[20] T. Zhang, X. F. Mo, Z. F. Han, and G. C. Guo, "Extensible router for multi-user quantum key distribution network," 2006.

[21] P. P. Yupapin and S. Mitatha, "Multi-users quantum key distribution via wavelength routers in an optical network," **Recent Patents on Computer Science**, vol. 2, no. 1, 2009, pp. 14–20.

[22] E. Waks, A. Zeevi, and Y. Yamamoto, "Security of quantum key distribution with entangled photons against individual attacks," **Phys. Rev. A**, vol. 65, 2002, p. 052310.

[23] S. Suchat, W. Khannam, and P. P. Yupapin, "Quantum key distribution via an optical wireless communication link for telephone networks," **Opt. Eng.**, vol. 46, 2007, p. 100502-1.

[24] M. Pfennigbauer, M. Aspelmeyer, W. Leeb, G. Baister, T. Dreischer, T. Jennewein, G. Neckamm, J. Perdigues, H. Weinfurter, and A. Zeilinger, "Satellite-based quantum communication terminal employing state-of-the-art technology," **J. Opt. Netw.**, vol. 4, 2005, p. 549.

[25] H. Takesue, S. W. Nam, Q. Zhang, R. H. Hadfield, T. Honjo, K. Tamaki, and Y. Yamamoto, "Quantum key distribution over 40 dB channel loss using superconducting single photon detectors," **Nat. Photon.**, vol. 1, 2007, p. 343.

[26] P. P. Yupapin, P. Phiphithirankarn, and S. Suchat, "A quantum CODEC design via an optical add/drop multiplexer in a fiber optic network," **Far East J. Electron. Commun.**, vol. 1, 2007, p. 259.

[27] Z. L. Yuan and A. J. Shields, "Continuous operation of a one-way quantum key distribution system over installed telecom fibre," **Opt. Exp.**, vol. 13, 2005, p. 660.

[28] B. Qi, "Single-photon continuous-variable quantum key distribution based on the energy–time uncertainty relation," **Opt. Lett.**, vol. 31, 2006, p. 2795.

[29] C. H. Bennett, G. Brassard, C. Crepeau, R. Jozsa, A. Peres, and W. K. Wootters, "Teleportingan unknown quantum state via dual classical an Einstein–Podolsky–Rosen," **Phys. Rev. Lett.**, vol. 70, 1993, pp. 1895–1899.

[30] E. Kreyzig, "**Introductory Functional Analysis with Applications.**" Wiley, New York, 1978.

[31] K. Mattle, H. Weinfurter, P. G. Kwiat, and A. Zeilinger, "Dense coding in experimental quantum communication," **Phys. Rev. Lett.**, vol. 76, 1996, pp. 4656–4659.

[32] P. P. Yupapin and S. Suchat, "Entangled photon generation using fiber optic Mach–Zehnder interferometer incorporating the nonlinear effect in a fiber ring resonator," **J. Nanophotonics**, vol. 1, 2007, p. 013504.

[33] P. P. Yupapin, P. Saeung, and C. Li, "Characteristics of complementary ring-resonator add/drop filters modeling by using graphical approach," **Opt. Commun.**, vol. 272, 2007, pp. 81–86.

[34] S. Suchat, W. Khannam, and P. P. Yupapin, "Quantum key distribution via an optical wireless communication link for telephone network," **Opt. Eng.**, vol. 46, no. 10, 2007, pp. 100502–100511.

[35] T. S. Manderbach, H. Weier, M. Furst, R. Ursin, F. Tiefenbacher, T. Scheidl, J. Perdigues, Z. Sodnik, C. Kurtsiefer, J. G. Rarity, A. Zeilinger, and H. Weinfurter, "Experimental demonstration of free-space decoy-state quantum key distribution over 144 km," **Phys. Rev. Lett.**, vol. 98, 2007, p. 010504.

[36] C. Fietz and G. Shvets, "Nonlinear polarization conversion using microring resonators," **Opt. Lett.**, vol. 32, no. 12, 2007, pp. 1683–1685.

[37] Dominik G. Rabus, "**Realization of Optical Filters using Ring Resonators with integrated Semiconductor Optical Amplifiers in GaInAsP / InP**".

[38] R. W. Boyd, "**Nonlinear Optics 2nd ed.**" Academic Press, Inc., 2003.

[39] M. F. Ferreira, "Optical solitons in fibers for communication systems," **Fiber Integrat. Optics**, vol. 24, 2005, pp. 287-314.

[40] A. Hasegawa (Ed.), "**New Trends in Optical Soliton Transmission Systems.**" AH Dordrecht, The Netherlands: Kluwer Academic Publishers, 1998.

[41] G. P. Agrawal, "**Fiber-Optic Communication Systems, 3rd ed.**" New York :Wiley , 2002.

[42] G. P. Agrawal, "**Nonlinear Fiber Optics, 4th ed.**" New York : Academic Press, 2007.

[43] Fan Yi Lin and Meng Chiao Tsai, "Chaotic communication in radio over fiber transmission based on optoelectronic feedback semiconductor laser," **Opt Exp.**, vol. 15, no. 2, Jan 2007, pp. 302-311.

[44] K. Ikeda, H. Daido, and O. Akimoto, "Optical turbulence: Chaotic behavior of transmitted light from a ring cavity," **Phys. Rev. Lett.**, vol. 45, 1980, pp. 709-712.

[45] D. A. B. Miller, S. D. Smith, and A. Johnston, "Optical bistability and signal amplification in a semiconductor crystal: Applications of new low-power nonlinear effects in InSb," **Appl. Phys Lett.**, vol. 35, no. 12, 1979, pp. 658–660.

[46] P. Mandel, S. Smith, and B. Wherrett, "**From Optical Bistability Towards Optical Computing.**" North-Holland, 1987.

[47] H. M. Gibbs, "**Controlling Light with Light.**" Academic Press Inc., 1985.

[48] K. Otsuka, "Pitchfork bifurcation and all-optical digital signal processing with a coupled-element bistable system," **Opt. Lett.**, vol. 14, no. 1, 1989. pp. 72-74.

[49] L. M. Zhao, D. Y. Tang, F. Lin, and B. Zhao, "Observation of period-doubling bifurcations in a femtosecond fiber soliton laser with dispersion management cavity," **Opt. Exp.**, vol. 12, no. 19, 2004, pp. 4573-4578.

[50] J. Ohtsubo, "Chaos Synchronization and Chaotic Signal Masking in Semiconductor Lasers With Optical Feedback," **IEEE J. of Quantum Electronics**, Vol. 38, No. 9, 2002, pp. 1141-1154.

[51] C. Juang, T. M. Hwang, J. Juang, and Wen-wei Lin, "A Synchronization Scheme using self-pulsating laser diode in optical chaotic communication," **IEEE J. Quantum Electron.**, Vol. 36, 2000, pp. 300-304.

[52] F. Y. Lin and M. C. Tsai, "Chaotic communication in radio over fiber transmission based on optoelectronic feedback semiconductor laser," **Opt Exp.**, vol. 15, no. 2, January 2007, pp. 302-311.

[53] K. Ikeda, H. Daido, and O. Akimoto, "Optical turbulence: Chaotic behavior of transmitted light from a ring cavity," **Phys. Rev. Lett.**, vol. 45, 1980. pp. 709-712.

[54] A. Hasegawa and Y. Kodama, "Signal transmission by optical solitons in monomode fiber," **Proc. IEEE.**, vol. 69, no. 9, Sept 1981, pp. 1145–1150.

[55] S. Blair, "**Optical soliton-based logic gates.**" Ph.D. dissertation, University of Colorado, 1998.

[56] E. Infeld and G. Rowlands, "**Nonlinear waves solitons and chaos.**" Cambridge university press, 2000.

[57] E. A. J. Marcatili, "Dielectric Rectangular Waveguide and Directional Coupler for Integrated Optics," **Bell. Syst. Tech. J.**, vol. 48, September 1969, pp. 2071-2101.

[58] C. K. Madsen and J. H. Zhao, "A General Planar Waveguide Autoregressive Optical Filter," **IEEE J. Lightwave Tech.**, vol. 14, no. 3, March 1996, pp. 437-447.

[59] S. C. Hagness, D. Rafizadeh, S. T. Ho, and A. Taflove, "FDTD Microcavity Simulations: Design and Experimental Realization of Waveguide-Coupled Single-Mode Ring and Whispering-Gallery-Mode Disk Resonators," **IEEE J. Lightwave Tech.**, vol. 15, no. 11, November 1997, pp. 2145-2165.

[60] D. Rafizadeh, J. P. Zhang, S.C. Hagness, A. Taflove, K. A. Stair, and S. T. Ho, "Waveguide-coupled AlGaAs/GaAs microcavity ring and disk resonators with high finesse and 21.6 nm free spectral range," **Opt. Lett.**, vol. 22, no. 16, August 1997, pp. 1244-1246.

[61] B. E. Little, J. S. Foresi, G. Steinmeyer, E. R. Thoen, S. T. Chu, H. A. Haus, E. P. Ippen, L. C. Kimerling, and W. Greene, "Ultra-Compact Si-SiO2 Microring resonator Optical Channel Dropping Filters." **IEEE Photon. Techn. Lett.**, vol. 10, no. 4, April 1998, pp. 549-551.

[62] D. J. W. Klunder, E. Krioukov, F. S. Tan, T. van der Veen, H. F. Bulthuis, G. Sengo, C. Otto, H. J. W. M. Hoekstra, and A. Driessen, "Vertically and laterally waveguide-coupled cylindrical microring resonators in Si3N4 on SiO2 technology." **Appl. Phys. B.**, vol. 73, no. 5-6, October 2001, pp. 603-608.

[63] B. Vanderhaegen et al., "High Q GaInAsP ring resonator filters," **ECIO'99**, Torino Italy, April 1999, pp. 381-384.

[64] M. K. Chin et al., "GaAs Microcavity Channel-Dropping Filter based on a Race-Track Resonator," **IEEE Photon. Techn. Lett.**, vol. 11, no. 12, December 1999, pp. 1620-1622.

[65] C. K. Madsen and J. H. Zhao, **"Optical Filter Design and Analysis: A Signal Processing Approach."** New York: Wiley, 1999.

[66] Kirankumar R. Hiremath, **"Coupled mode theory based modeling and analysis of circular optical microresonators."**, 2005.

[67] H. van de Stadt, "Ring interferometers with unit transmittance," **Appl. Opt.**, vol.24, 1985, pp. 2290-2292.

[68] C. K. Madsen, G. Lenz, A. J. Bruce, M. A. Capuzzo, L. T. Gomez, T. N. Nielsen, and I. Brener, "Multistage dispersion compensator using ring resonators," **Opt. Lett.**, vol. 24, 1999, pp. 1555–1557.

[69] C. K. Madsen, G. Lenz, A. J. Bruce, M. A. Capuzzo, L. T. Gomez, and R. E. Scotti, "Integrated all-pass filters for tunable dispersion and dispersion slope compensation," **IEEE Photon. Technol. Lett.**, vol. 11, 1999, pp. 1623–1625.

[70] G. Lenz and C. K. Madsen, "General optical all-pass filter structures for dispersion control in WDM systems," **J. Lightwave Technol.**, vol. 17, 1999, pp. 1248–1254.

[71] C. K. Madsen, "Optical all-pass filters for polarization mode dispersion compensation," **Opt. Lett.**, vol. 25, 2000, pp. 878–880.

[72] R. Ramaswami and K. N. Sivarajan, **"Optical Networks: A Practical Perspective."** San Francisco, CA : Morgan Kaufmann, 1998.

[73] M. D. Lukin and A. Imamoglu, "Controlling photons using electromagnetically induced transparency," **Nature**, vol. 413, September 2001, pp. 273-276.

[74] L. M. Duan, M. D. Lukin, J. I. Cirac, and P. Zoller, "Long-distance quantum communication with atomic ensembles and linear optics," **Nature**, vol. 414, November 2001, pp. 413-418.

[75] M. F. Yanik and S. Fan, "Stopping light all optically," **Phys. Rev. Lett.**, vol. 92, 2004, p. 083901.

[76] M. F. Yanik and S. Fan, "Stopping and storing light coherently," **Phys. Rev. A**, vol. 71, 2005, p. 013803.

[77] P. P. Yupapin, N. Pornsuwanchroen, and S. Chaiyasoonthorn, "Attosecond pulse generation using nonlinear micro ring resonators," **Microw. and Opt. Technol. Lett.**, vol. 50, no. 12, 2008, pp. 3108-3111.

[78] C. Fietz and G. Shvets, "Nonlinear polarization conversion using micro ring resonators," **Opt. Lett.**, vol. 32, 2007, p. 1683.

[79] Y. Kokubun, Y. Hatakeyama, M. Ogata, S. Suzuki, and N. Zaizen, "Fabrication technologies for vertically coupled micro ring resonator with multilevel crossing bus line and ultracompact ring radius," **IEEE J. of Selected Topics in Quantum Electron.**, vol. 11, no. 1, 2005, pp. 4-10.

[80] Y. Su, F. Liu and Q. Li, "System performance of show-light buffering and storage in silicon nano-waveguide," **Proc. SPIE**, vol. 6783, 2007, p. 67832.

[81] M. Takikuchi, Y. Yoshikawa, Y. Yamariku, Y. Toril, and T. Kuga, "**Fabrication of Nano-fiber Resonators, for Single-Atom Detection.**" Institute of Physics, University of Tokyo, 2007.

[82] D. Anderson, "Optical filters fill many roles," **WDM Solutions**, June 2001, pp. 97-99.

[83] S. Kempainen, "Optical networking lightens carrier-backbone burden," **EDN, www.ednmag.com**, vol. 8, October 1998, pp. 63-72.

[84] E. Pawlowski et al., "Fabrication of a multichannel Wavelength-division multiplexing passive optical net demultiplexer with arrayed waveguide gratings and diffractive iptical elements," **Appl. Optics**, vol. 38, no. 14, 1999, pp. 3039-3045.

[85] S. Suchat, W. Khannam, and P. P. Yupapin, "Quantum key distribution via an optical wireless communication link for telephone networks," **Opt. Eng.**, vol. 46, no. 10, 2007, p. 100502-1.

[86] P. P. Yupapin and S. Suchat, "Entangled photon generation using a fiber Optic Mach-Zehnder interferometer incorporating the nonlinear effect in a fiber ring resonator," **J. of Nanophotonics.**, vol. 1, 2007, p. 013504.

[87] P. P. Yupapin, P. Phiphithirankarn, and S. Suchat, "A quantum CODEC design via an optical add/drop multiplexer in a fiber optic network," **Far East Journal of Electron. and Commun.**, vol. 1, 2007, p. 259.

[88] P. Trojek, Ch. Schmid, M. Bourennane, and H. Weinfurter, "Compact source for polarization entangled photon pairs," **Opt. Exp.**, vol. 12, 2004, p. 276.

[89] S. Suchat, W. Khunnam, and P. P. Yupapin, "Entangled photons generation and recovery using a fiber ring resonator incorporating an erbium doped fiber amplifier," **Opt. Eng.**, vol. 46, no. 7, 2008, p. 100502-1.

[90] C. Fietz and G. Shvets, "Nonlinear polarization conversion using micro ring resonators," **Opt. Lett.**, vol. 32, 2007, p. 1683.

[91] H. Takesue, K. Inoue, O. Tadanaga, Y. Nishida, and M. Asobe, "Generation of pulsed polarization-entangled photon pairs in a 1.55 micrometer band with a periodically poled lithium niobate waveguide and an orthogonal polarization delay circuit," **Opt. Lett.**, vol. 30, 2005, p. 293.

[92] Z. Yang, P. Chak, A. D. Bristow, and H. M. van Driel, "Enhanced second-harmonic generation in AlGaAs micro ring resonators," **Opt. Lett.**, vol. 32, 2007, p. 826.

[93] P. P. Yupapin and W. Suwancharoen, "Chaotic signal generation and cancellation using a micro ring resonator incorporating an optical add/drop multiplexer," **Opt. Commun.**, vol. 280, 2007, p. 343.

[94] P. P. Yupapin and W. Suwanchroen, "**A novel technology for mobile telephone networks and security.**" Mobile Telephones: Networks, Applications, and Performance, Editors: Alvin C. Harper and Raymond V. Buress, Nova Science Publishers : ISBN: 978-1-60456-436-5, 2008.

[95] P. P. Yupapin and P. Chunpang, "A Quantum-chaotic encoding system using an erbium-doped fiber amplifier in a fiber ring resonator," **International Journal of Light and Electron Optics**, vol. 120, no. 18, December 2009, pp. 976-979.

[96] W. Khunnam and P. P. Yupapin, "An investigation of the entangled photon walk-off compensation generated by a fiber ring resonator," **International Journal of Light and Electron Optics**, vol. 120, no. 14. September 2009, pp 731-735.

[97] S. Chaiyasoonthorn, S. Mitatha, K. Dejhan, and P. P. Yupapin, "Attosecond pulse and its beyond generation based on multi-stage micro ring resonators," **J. Adv Mater. Res.**, vol. 55–57, 2008, pp. 485–488.

[98] C. Silberhorn, P. K. Lam, O. Weib, F. Konig, N. Korolkova, and G. Leuchs, "Generation of continuous variable Einstein-Podolsky-Rosen entanglement via the Kerr nonlinearity in an optical fiber," **Phys. Rev. Lett.**, vol. 86, 2001, pp. 4267-4270.

[99] C. H. Bennett, G. Brassard, C. Crepeau, R. Jozsa, A. Peres, and W. K. Wootters, "Teleporting an unknown quantum state via dual classical an Eistein–Podolsky–Rosen," **Phys. Rev. Lett.**, vol. 70, 1993, pp. 1895–1899.

[100] K. Mattle, H. Weinfurter, P. G. Kwiat, and A. Zeilinger, "Dense coding in experimental quantum communication," **Phys. Rev. Lett.**, vol. 76, 1996, pp. 4656–4659.

[101] P. P. Yupapin and S. Suchat, "Entangled photon generation using fiber optic Mach–Zhender interferometer incorporating the nonlinear effect in a fiber ring resonator," **J. Nanophotonics**, vol. 1, 2007, p. 013504.

[102] S. Suchat, W. Khannam, and P. P. Yupapin, "Quantum key distribution via an optical wireless communication link for telephone network," **Opt. Eng.**, vol. 46, 2007, pp. 100501–100502.

[103] P. P. Yupapin, P. Phiphithirankarn, and S. Suchat, "A quantum CODEC design via an optical add/drop multiplexer in a fiber optic network," **Far East J. Electron. Commun.**, vol. 1, 2007, pp. 259–267.

[104] C. Fietz and G. Shvets, "Nonlinear polarization conversion using micro ring resonators," **Opt. Lett.**, vol. 32, 2007, pp. 1683–1685.

[105] P. P. Yupapin and N. Pornsuwancharoen, "Proposed nonlinear micro ring resonator arrangement for stopping and storing light," **IEEE Photon. Technol. Lett.**, vol. 21, no. 6, March 2009, pp. 404-406.

[106] P. P. Yupapin, S. Thongmee, and K. Sarapat, "Second-harmonic generation via micro ring resonators for optimum entangled photon visibility," **Int. J. Light Electron Opt., vol. 121, no. 7**, April 2010, pp. 599-603.

[107] P. P. Yupapin, "Generalized quantum key distribution via micro ring resonator for mobile telephone networks," **Int. J. Light Electron Opt.**, vol. 121, no. 5, March 2010, pp. 422-425.

[108] G. Stewarta, "A safety approach to information security communications," **Inf. Secur. Technol. Rep.**, vol. 14, no. 4, 2009, pp. 197–201.

[109] Y. Pei, Y. C. Liang, L. Zhang, K. C. Teh, and K. H. Li, "Secure communication over MISO cognitive radio channels," **IEEE Trans. Wireless Comm.**, vol. 9, no. 4, 2010, pp. 1494–1502.

[110] J. Dong, K. Ackermann, and C. N. Rotaru, "Secure group communication in wireless mesh networks," **Ad Hoc Netw.**, vol. 7, no. 8, 2009, pp. 1563–1576.

[111] X. Y. Wang and Y. F. Gao, "A switch-modulated method for chaos digital secure communication based on user-defined protocol," **Commun. Nonlin. Sci. Numer. Simul.**, vol. 15, no. 1, 2010, pp. 99–104.

[112] X. M. Xiu, H. K. Dong, L. Dong, Y. J. Gao, and F. Chi, "Deterministic secure quantum communication using four-particle genuine entangled state and entanglement swapping," **Opt. Commun.**, vol. 282 , no. 12, 2009, pp. 2457–2459.

[113] L. Dong, X. M. Xiu, Y. J. Gao, and F. Chi, "Deterministic secure quantum communication against collective-dephasing noise by using EPR pairs and auxiliary photons," **Opt. Commun.**, vol. 282, no. 8, 2009, pp. 1688–1690.

[114] A. Sinha, H. Bhowmik, P. Kuila, and S. Mukhopadhyay, "New method of controlling the power of a Gaussian optical pulse through an electro-optic modulator and a nonlinear waveguide for generation of solitons," **Opt. Eng.**, vol. 44, no. 6, 2005, p. 065003.

[115] Y. Y. Lin and R. K. Lee, "Dark-bright soliton pairs in nonlocal nonlinear media," **Opt. Exp.**, vol. 15, no. 14, 2007, pp. 8781–8786.

[116] S. Mitatha, N. Chaiyasoonthorn, and P. P. Yupapin, "Dark-bright optical solitons conversion via an optical add/drop filter," **Microw. Opt. Technol. Lett.**, vol. 51, 2009, pp. 2104–2107.

[117] N. Pornsuwancharoen, U. Dunmeekaew, and P. P. Yupapin, "Multi-soliton generation using a micro ring resonator system for DWDM based soliton communication," **Microw. and Opt. Technol. Lett.**, vol. 51, 2009, pp. 1374–1377.

[118] S. F. Hanim, J. Ali, and P. P. Yupapin, "Dark soliton generation using dual Brillouin fiber laser in a fiber optic ring resonator," **Microw. Opt. Technol. Lett.**, vol. 52, 2010, pp. 881–883.

[119] J. Ali and P. P. Yupapin, "An experimental investigation of multisoliton generation using an erbium-doped fiber amplifier and a fiber optic ring resonator," **Microw. Opt. Technol. Lett.**, vol. 52, 2010, pp. 70–72.

[120] S. Roy, S. K. Bhadra, and G. P. Agrawal, "Perturbation of higher-order solitons by fourth-order dispersion in optical fibers," **Opt. Commun.**, vol. 282, 2009, pp. 3798–3803.

APPENDIX

LIST OF PUBLICATIONS

Publication in 2011

1. P. Yooplao, P. Pongwongtragull, S. Mitatha, and P. P. Yupapin, "Crosstalk effects of quantum key distribution via a quantum router," **Microw. and Opt. Technol. Lett.**, vol. 53, no. 5, May 2011, pp. 1094-1099. (Impact Factor:2010:0.656)

2. P. Pongwongtragull, C. Teeka, S. Kamoldilok, and P.P. Yupapin, "Novel communication security scheme using dark-bright soliton conversion behaviors," **Opt. Eng.**, vol.50, no.2, February 2011, pp. 25004-25004. (Impact Factor:2010:0.815)

Publication in 2010

1. P. Pongwongtragull, S. Mitatha, and P.P. Yupapin, "A simultaneous generation of QKD and QDC via optical memory array for distributed network security," **Int. J. Light Electron Opt.**, vol. 121, no. 23, December 2010, pp. 2137-2139. (Impact Factor: 2010:0.454)

2. P. Pongwongtragull, S. Suchat, S. Mitatha, and P. P. Yupapin, "Quantum parallel processing manipulation using gaussian pulses via an optical multiplexer," **Progress In Electromagnetics Research Symposium Proceedings**, Xi'an, China, March 22-26, 2010, pp. 1689-1693.

BIOGRAPHY

Name: Mr.Paiboon Pongwongtragull

Date of Birth: April 8th , 1974

Born: Songkhla, Thailand.

Current Address: 79/193 Thanon Sangkha Pracha, Lam Phakchi, Nong Chok, Bangkok, Thailand, 10530.

E-mail: kppaiboo@kmitl.ac.th.

Education

- Bachelors of Science in Industrial Education (Electronics and Computer) from King Mongkut's Institute of Technology Ladkrabang Bangkok, Thailand, in 1996.

- Master of Engineering in Electrical Engineering from King Mongkut's Institute of Technology North Bangkok (KMIT'NB), Thailand, in 2003.

Skilled Works

- Computer Programming and Electronics
- Optics Communications
- Fiber Optics, Nonlinear Optic and Simulation
- Quantum Communications and Parallel Processing